UPPSALA
UNIVERSITET

An evaluation of an MBBR anammox model - sensitivity analysis and calibration

Clara Jonfelt

Abstract

An evaluation of an MBBR anammox model - sensitivity analysis and calibration

Clara Jonfelt

This master thesis is about mathematical modelling of the anammox process with a moving bed biofilm reactor (MBBR) for a reject water application. Specifically, the aim of my research was to find out whether the model proposed by Erik Lindblom in (Lindblom et al. 2016) is a good model for this purpose and worth continuous research and optimization.

The code for the model, implemented in Matlab/Simulink, was given; although not initially functioning in the given condition. Some modifications needed to be done to make it function properly. In order to confirm that the code was working and used in a correct way some results in (Lindblom et al. 2016) were reproduced. Before starting the evaluation of the model, some much-needed optimizations of the code were done, substantially reducing the run time.

A sensitivity analysis was done, and the five most sensitive parameters were picked out to be used in the calibration. The calibration improved the total fit of the model to the available measurements, although one of the model outputs could not be calibrated satisfactorily.

In short, I found that although there are still problems left to solve before the model can be stated to accurately model the anammox process with MBBR, it appears promising. Most importantly, more measurement data are needed in order to make a proper validation and to do a better calibration.

Populärvetenskaplig sammanfattning

Det moderna samhället är beroende av väl fungerade vattenrening. Om allt vårt avloppsvatten skulle släppas ut orenat skulle den omgivande miljön snabbt förorenas. Forskning i syfte att förbättra de processer som finns i vattenreningsverk pågår ständigt. Nya och hårdare miljökrav samt möjlighet till kostnadsbesparingar motiverar förbättringar av redan existerande processer och forskning på nya, inovativa metoder.

Ett av de ämnen man kan avskilja i ett vattenreningsverk är kväve. Kväverening utförs med biologiska metoder där mikroorganismer, framförallt bakterier, omvandlar kvävet i avloppsvattnet, som är i form av ammonium, till kvävgas som går upp i luften. På detta sätt undviks att kvävet släpps ut i sjöar och hav, där det kan orsaka övergödning. *Anammox* är en relativt ny, alternativ metod för kväverening i vattenreningsverk. Den har ett flertal fördelar jämfört med traditionell kväverening, bl.a. har den lägre energiförbrukning och genererar mindre växthusgaser. Anammox kan användas i en s.k. Moving Bed Biofilm Reactor (MBBR) där biomassa växer på bärare i plast i en tank. Metoden har med framgång implementerats i rejektvattenströmmar vid reningsverk. En rejektvattenström är en sidoström i ett vattenreningsverk som kommer från avvattning av slam. Den har hög temperatur och hög kvävekoncentration - ideala förhållanden för anammox-processen. Liksom i övriga samhället har utsläpp av växhusgaser och andra miljöaspekter fått mer och mer fokus vid vattenreningsverk. Att t.ex. minska utsläpp av växthusgaser och minimera energiförbrukningen, är också viktiga aspekter att ta hänsyn till när kväverenngsssteget utformas, förutom en hög kväveavskiljningsgrad.

Erik Lindblom (Stockholm Vatten) har utformat en matematisk modell som modellerar anammox med MBBR i rejektvattenströmmar. Den bygger huvudsakligen på de välanvända Activated Sludge Models (ASM), skapade av International Water Association (IWA), som beskriver hur ämnen rör sig och omvandlas i en aktivslam-anläggning. Modellen har sedan utökats med andra modeller som behövs för att simulera anammox med MBBR; bl.a. en modell för den biofilm som byggs upp på bärarna.

Med hjälp av matematisk modellering kan man få kunskap om systemets dynamik, något som är en förutsättning för att på ett bra sätt kunna styra den process som sker i systemet. Man kan också göra fler försök än vad som i verkligheten är praktiskt möjligt och enkelt undersöka hur olika förhållanden påverkar processen. Anammox-processen har långsam tillväxthastighet vilket gör att uppstartstiden är lång och processen sker långsamt; med en modell kan förloppet snabbspolas".

Den här masteruppsatsen handlar om matematisk modellering av anammox-processen med Moving Bed Biofilm Reactor (MBBR) för en rejektvattentillämpning. Det specifika målet för arbetet var att ta reda på om modellen, föreslagen av Erik Lindblom i (Lindblom m. fl. 2016), är en tillräckligt bra modell för att kunna användas i vidare utveckling.

Koden för modellen, implementerad i Matlab/Simulink, var given. Dock fungerade den inte så som den ursprungligen såg ut och några ändringar behövde göras för att få den att fungera ordentligt. För att kontrollera att den modifierade koden fungerade som den skulle och användes på rätt sätt reproducerades några resultat från (Lindblom m. fl. 2016). Innan utvärderingen av modellen påbörjades gjordes också några välbehövliga optimeringar av koden, vilka avsevärt reducerade körtiden.

En känslighetsanalys gjordes, och de fem känsligaste parametrarna valdes ut för att användas vid kalibreringen. Kalibreringen förbättrade den totala anpassningsgraden för modellen till den tillgängliga mätdatan. En av modellens utdata-parametrar kunde dock inte kalibreras tillfredställande.

Även om det finns problem med modellen kvar att lösa innan den kan konstateras modellera anammox-processen tillförlitligt så anser jag att den verkar den lovande. Viktigast är att få tillgång till mer mätdata för att kunna göra en ordentlig validering av modellen och en bättre kalibrering.

Acknowledgments

Abbreviations

N_2O	nitrous oxide
N_2	nitrogen gas
NH_3	ammonia
NH_4^+	ammonium
NO_2^-	nitrite
NO_3^-	nitrate
NO	nitric oxide
AMX	anammox
AOB	ammonia-oxidizing bacteria
ASM	activated sludge model
ASP	activated sludge process
COD	chemical oxygen demand
d	days
DO	dissolved oxygen
FA	free ammonia
FNA	free nitrous acid
HNO2	nitrous acid
MBBR	moving bed biofilm reactor
N	nitrogen
NOB	nitrite oxidizing bacteria
OAT	one-at-a-time
S	soluble component
X	particulate component

Contents

List of Figures

List of Tables

Chapter 1

Introduction

This project is part of a project named CONAN, which has PURAC, Mälardalen University (MdH), and ABB as partners. In addition, it has had three years of economic support from Vinnova, reference number (2015-02422). The aim of CONAN is to develop a control system for the one-step deammonification technique - anammox with MBBR, for a reject water application. The main priorities for this control system are that it should provide: stability, reliability during start-up without anammox seeding, high nitrogen reduction efficiency, energy efficiency, and low nitrous oxide emissions.

1.1 Background

A well functioning wastewater treatment is essential for modern society. Without it the surrounding environment would soon become subject to a number of serious environmental complications. Emissions of nutrients, oxygen-consuming substances, and toxic substances pollute waters surrounding cities. Euthrophication is one such example; it is caused by addition of phosphorus and nitrogen beyond the natural levels. In the 1960s, knowledge about euthrophication gained attention as it was happening all over Sweden. Also, decades of unregulated emissions in larger cities had adversely affected the environment. Consequently, in the 1970s, initiatives were taken to substantially expand and construct wastewater treatment plants all over the country. Nitrogen reduction in wastewater plants was introduced in the mid 80s. (Naturvårdsverket 2014)

The main sources of additive amounts of phosphorus and nitrogen - causing eutrophication - in Sweden today are leaching from arable land and emissions from wastewater treatment plants. Wastewater plants whose recipient water is Skagerack, Kattegat, Öresund, or the Baltic Sea have trouble with these waters' vulnerability to nitrogen emission – which is part of what contributes to euthropication; particularly in the Baltic Sea where it is currently at a dire level. In addition, Sweden has so far been unable to meet the 2014 EU environmental demands to lower nitrogen emissions to the agreed level – thereby halting the euthropication. Also, as in the rest of society, a more substantial focus has been put on energy consumption and carbon dioxide footprints in the wastewater treatment plants. In the light of this, nitrogen removal techniques is a current and relevant field of scientific research for a prosperous sustainable future. (Naturvårdsverket 2014)

Conventional nitrogen removal in wastewater treatment has used *nitrification/denitrification*, which is a biological process through which nitrogen is converted from ammonium to nitrogen gas. This wastewater treatment method has limits, such as a need for an external carbon source - like methanol. In addition, in comparison to other ways to remove nitrogen, this method consumes high levels of energy, mainly due

to the vast aeration needed in order to provide enough oxygen for the process to be successful. (Star 2008)

Modern society is always looking for improvement and progress; such is the fate of wastewater treatment, which, like many other areas of society, continuously strive to overcome problems and to meet new environmental requirements. An alternative to nitrification/denitrification that has been discovered is a process called *anammox* - an acronym for anaerobic ammonium oxidation. Its benefits in comparison to nitrification/denitrification are feats such as that: (1) it is not dependent on an external carbon source, (2) less aeration is needed, and (3) subsequently, it lowers the cost of the energy required for the wastewater treatment process. Also, less greenhouse gases are emitted when anammox is used. (Star 2008)

Internal plant recycle side-streams from dewatering of sludge - reject water, has a high temperature and a high COD/N-ratio - ideal conditions for the anammox process. Full-scale implementations of anammox have already been made in these side-stream processes in several countries. Preferably, it ought to be used in mainstream processes too. What hinders that from becoming reality is mainly that the mainstream has lower temperatures and lower N/COD-ratio, which makes it difficult for an anammox process to be established.

There is a wide range of usefulness and purposes with modelling a system. Modelling provides insight and knowledge about the dynamics of the system we aim to control, thereby enabling the construction of controlling devices. The process of modelling reduces the number of practical experiments and investigates all variations possible; modelling allows us to try a large number of constellations in the wastewater treatment process. Also, since the anammox process has a long start-up time, a model can help fast-forward the process, and put to the test hypotheses impossible to practically test in reality. Through modelling, we can try out and implement theories as well as combine different models describing different aspects and processes related to the wastewater treatment process. Furthermore, it can be helpful when trying to operate and optimize an ongoing wastewater treatment process as it helps us to predict, to some extent, the process behavior. Also, there is an educational side-effect to the development of models since they can lead to a better understanding of the process as such, making visible the previously invisible. A good mathematical model can thus be very helpful in further development of the one-step anammox process with MBBR.

1.2 Objective

The objective of this project is to investigate the model of the one-step anammox process with MBBR, proposed by Erik Lindblom in (Lindblom et al. 2016) and prove or disprove whether it would be a good basis for further development of a model for the anammox process. The model will be implemented in the software Matlab/Simulink.

The main steps of this project will be to: 1) reproduce the results in figure 3 of the MBBR anammox given by (Lindblom et al. 2016), which is obtained with the model, 2) find the most sensitive parameters with a sensitivity analysis, and 3) calibrate the model with respect to the most sensitive parameters. Some suggestions regarding improvements will be made if possible.

Chapter 2

Theory - The biological system

In this chapter, the theory about the biological system that forms the basis for the one-step anammox with MBBR is reviewed. A general overview of wastewater treatment, especially the biological wastewater treatment, is given and followed by a more detailed review about the techniques to be modelled.

2.1   Wastewater treatment

A combination of mechanical, chemical and biological treatments are used in wastewater treatment in Sweden. In the mechanical treatment, coarse and fine solids are removed with screens, sand-traps and primary sedimentation. In the chemical treatment primarily phosphorous are separated from the wastewater by the addition of reagents, approximately removing 90 % of the phosphorus. The biological treatment is described in the following section. (Naturvårdsverket 2014)

2.2   Biological wastewater treatment

In biological wastewater treatment, microorganisms, mostly bacteria, decompose organic waste, for example carbon and nitrogen compounds, through digestion of the organic material. Activated sludge process (ASP) is the most widely used biological wastewater treatment method. The term 'activated sludge' refers to the fact that natural processes of the microorganisms in the sludge are accelerated through the maintenance of ideal conditions. The microorganisms gather into biomass flocks and are kept suspended in the wastewater. The biomass suspension is kept in an aerated tank since the organisms consume oxygen as they oxidize the organic matter for growth and energy. The biomass flocks are then separated from the treated water in a settle and re-circulated in order to retain biomass in the system. ASP can, depending on the design, remove organic carbon substance, phosphorus, and nitrogen. (Naturvårdsverket 2014)

2.3   Moving bed biofilm reactor (MBBR)

An alternative to ASP that has been developed based on the same process, is the moving bed biofilm reactor (MBBR) technique. In an MBBR, a biofilm is made up of microorganisms that grow on suspended plastic carriers with a large protected surface area, see Figure 2.1. The large area containing concentrated biomass makes MBBR space efficient. Furthermore, a settler is not needed in order to keep the biomass in the system as long as the biofilm growth in the carrier is higher than the washout of the suspended

Figure 2.1: Carrier with anammox bacteria. Image source: The CONAN project

biomass in the bulk. The carriers in an MBBR have a density just below the density of water and are in continuous motion, mixed by the aeration in oxic (aerated) conditions or mechanically in anoxic (oxygen is only available as nitrate) conditions. In an MBBR, both oxic and anoxic conditions can be obtained in a single tank - oxic in the outer biofilm layers, closest to the bulk; and anoxic in the deeper layers, closest to the carrier. Substrates are transported between the bulk and the biofilm, driven by the gradient of concentrations. If a substrate is consumed within the biofilm, its gradient is directed from the bulk towards the biofilm; if the substrate is produced within the biofilm, the gradient is directed out from the biofilm towards the bulk. One limitation with the MBBR is that it is hard to remove >70% of the non-organic nitrogen without long retention times (<2 days) (Trela et al. 2008).

2.4 Nitrogen removal

Most of the incoming nitrogen in wastewater is in the form of ammonium, NH_4^+. When nitrogen removal is implemented at a wastewater treatment plant it is implemented in the biological step. It is commonly removed by a technique called nitrification/denitrification, but lately a technique called anammox has been brought into use in reject water streams. These two techniques will be reviewed in the following sections. It should be mentioned that nitrogen removal is comparatively complicated and therefore mostly implemented at larger plants or in places where the recipient is extra vulnerable.

2.4.1 Nitrification/denitrification

Conventionally, nitrogen is removed via nitrification of the ammonium to nitrite, NO_2^-, and then to nitrate, NO_3^-, followed by denitrification to nitrogen gas, N_2, see Figure 2.2. The first step is done by chemical autotrophic organisms as ammonia oxidizing bacteria (AOB) oxidize the ammonium to nitrite, and nitrite oxidizing bacteria (NOB) oxidize the nitrite to nitrate. It is an autotrophic process, using carbon dioxide as its carbon source. The stoichiometric reactions, without metabolism, for the nitrification processes are

$$NH_4^+ + 1.5\,O_2 \longrightarrow NO_2^- + 2\,H^+ + H_2O. \tag{2.1}$$

and

$$NO_2^- + 0.5\,O_2 \longrightarrow NO_3^-, \tag{2.2}$$
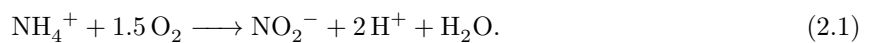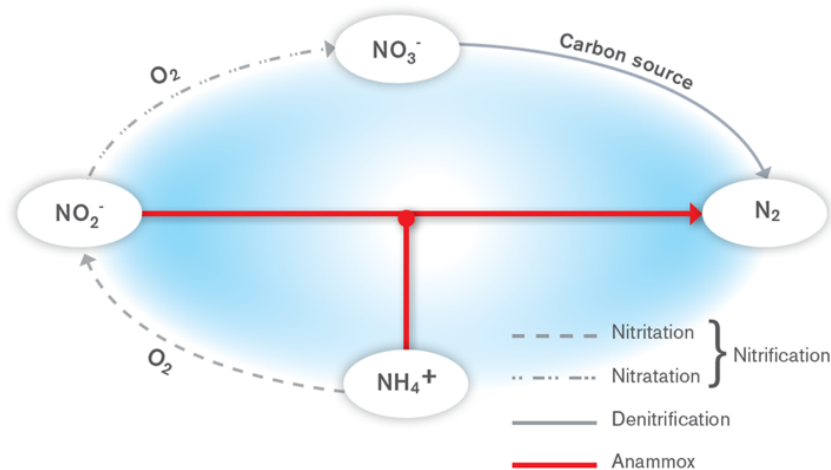
Figure 2.2: The nitrogen cycle. The pathways for nitrification, denitrification, and anammox are marked. Image source: The CONAN project

respectively. The denitrification of the nitrate to nitrogen gas is done by heterotrophic bacteria, using organic material as carbon source, and is an anoxic process. The carbon content in the wastewater is commonly not sufficient for the process and thus requires an additional, external carbon source, such as methanol or ethanol. If for example methanol, $5\,CH_3OH$, is used as carbon source, the stoichiometric reaction for the conversion of nitrate would be

$$6\,NO_3^- + 5\,CH_3OH \longrightarrow 2\,N_2 + 5\,CO_2 + 7\,H_2O + 6\,OH^-. \tag{2.3}$$
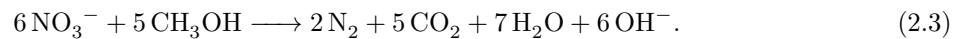
In this process, about 50-75% of the nitrogen is removed. (Naturvårdsverket 2014)

Nitrification/denitrification as a method for nitrogen removal has a few downsides: it produces excess sludge, it is highly energy consuming (mainly due to its high oxygen demand since both AOB and NOB need oxygen), and it also produces non-negligible quantities of green-house gases - mainly CO_2 and N_2O.

2.4.2 The anammox process

Anammox is an acronym for anaerobic ammonia oxidation. Discovered in the early 1990's (Kuenen 2008), it was not until 2011 that the reaction could be described thoroughly (Kartal et al. 2011). It is a fully autotrophic process.

The anammox process makes a kind of short-cut in the nitrogen cycle, shown in Figure 2.2, where ammonium together with nitrite is converted directly into nitrogen gas. A two-step process is required to convert ammonium into nitrogen gas in wastewater treatment plants for nitrogen removal: Partial nitrification followed by anammox (deammonification) - often simply called 'anammox' or 'the anammox process'. For these two steps, both oxic and anoxic conditions are required. These conditions can be achieved either by using a one-step biofilm method, such as the MBBR, or a two-step process with two tanks; one aerobic for the partial nitritation with AOB and one anaerobic for the anammox reaction. Less nitrous gas, N_2O, is produced with the MBBR than with a two-step method, probably because the nitrite is immediately consumed (Star 2008).

Partial nitrification

Partial nitrification is needed in order to convert ammonium into nitrogen gas with the anammox pathway. Approximately half of the ammonium should be oxidized into nitrite. Further oxidation of nitrite to nitrate should be barred in order to avoid the nitrogen from being converted to nitrogen gas along the nitrification/denitrification pathway. The reaction stoichiometry for the partial nitrification is as in equation 2.1.

Anammox/Deammonification

The nitrite from the partial nitrification is then used as the electron acceptor in a process where nitrite and ammonium is converted into nitrogen gas, shown in Figure 2.2. Carbon dioxide is used as the carbon source, as the process is autotrophic. It is reversibly inhibited by oxygen, but a low oxygen concentration can be tolerable if AOB is present, since AOB consume oxygen in the oxidation of ammonium to nitrite. Some nitrate is inevitably produced; if the process is fully autotrophic, the anammox growth process can be measured by the production rate of nitrate. Since the anammox process does not need oxygen, only about half of the oxygen is required for nitrogen removal with partial nitrification followed by anammox - as only half of the ammonium has to be oxidized to nitrite. The reaction stoichiometry, including metabolism, was first stated by (Strous et al. 1998) and is given by:

$$
\begin{aligned}
\mathrm{NH_4}^+ + 1.32\,\mathrm{NO_2}^- + 0.066\,\mathrm{HCO_3}^- + 0.13\,\mathrm{H}^+ &\longrightarrow \\
1.02\,\mathrm{N_2} + 0.066\,\mathrm{CH_2O_{0.5}N_{0.15}} + 0.26\,\mathrm{NO_3}^- + 2.03\,\mathrm{H_2O}
\end{aligned}
\tag{2.4}
$$
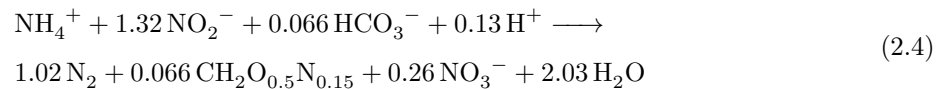
One of the main difficulties with the anammox process is to favor anammox and AOB, while at the same time disfavor NOB so that nitrification/denitrification is avoided. The competition about substrates is as follows: NOB and AOB both want oxygen, anammox and NOB want nitrite, and AOB and anammox want ammonium. At high temperatures, NOB can easily be outcompeted by anammox. At lower temperatures, oxygen control (oxygen level and aeration pattern) can be used as NOB is more inhibited at low oxygen levels than AOB. At higher ammonium concentrations, AOB outcompete NOB. At lower temperatures and ammonium concentrations, it is thus hard to avoid extensive oxidation of nitrite to nitrate by NOB. Because of this, anammox is currently only applied in full-scale to the ammonium-rich and relatively warm (20-35ºC) reject water stream - the effluent from the sludge digester that is to be recirculated in the main stream. Despite these facts, in nature, anammox reactions have been found at all temperatures. In fact, 30-50 % of the production of nitrogen gas in the seas comes from anammox reactions (Devol 2003).

The main benefits of using the anammox process instead of nitrification/denitrification are: (1) it saves oxygen and energy needed for aeration; (2) no external carbon source is needed; (3) less sludge is produced; (4) less carbon dioxide and nitrous oxide is released - $\mathrm{N_2O}$ is not an intermediate with anammox as with other denitrifying bacteria, since $\mathrm{N_2O}$ is a strong greenhouse gas this is great for sustainability; (5) biogas, $\mathrm{CH_4}$, can be produced from the sludge since the carbon sources in the wastewater are not needed for the nitrogen removal. Down-sides with using the anammox process are: (1) low growth rate; (2) low biomass production; (3) long start-up time.

Even though the anammox process has only so far been implemented in full scale in reject water streams, it plays an important role in lowering the nitrogen load in the main stream. To implement it in the main stream is hard, as the conditions there is not favorable for the anammox process. This is an ongoing area of research; from the results so far it appears promising (Plaza et al. 2015).

6

2.5 Aeration

Additional aeration is essential to the biological wastewater treatment as the microorganisms need enough oxygen to decompose organic substances. Also, oxygen is needed for some of the steps in the nitrogen removal treatment, described above. The aeration can be conducted either intermittent or constantly. Aeration is energy demanding, we thus want to minimize the air supply; still the concentration of dissolved oxygen (DO) is a key factor for both nitrification and denitrification. Consequently, DO is an important value that has to be set carefully and monitored continuously. The dynamics of the DO can be expressed as follows:

$$\frac{dC}{dt} = K_L a(C_S - C) - r_M + \frac{Q}{V}(C_{in} - C), \tag{2.5}$$

where $K_L a$ [d^{-1}] is the oxygen transfer coefficient and d is days, C [g/m^3] is the dissolved DO concentration, C_S [g/m^3] is the DO saturation concentration, r_M [g/(m^{3}d)] is the respiration rate of the microorganisms, Q [m^3/d] is the inflow, V [m^3] is the volume of the respiration tank, and C_{in} [g/m^3] is the influent DO concentration. $K_L a$ determines the rate of the oxygen transport from gaseous oxygen in the air into dissolved oxygen in the water. It contains aggregated information about the oxygen transfer efficiency under given conditions.

Intermittent aeration can be used to achieve both anoxic and oxic conditions in the same tank; at low oxygen levels anoxic conditions are created, and when the aeration is turned on oxic/aerobic conditions are created. Also, since AOB responds faster than NOB to increasing oxygen levels, AOB can be favored over NOB with intermittent aeration as long as there is sufficient ammonium available. Intermittent aeration can thus improve the anammox process; the anammox bacteria benefit from the non-aerated periods and the AOB get the required oxygen and can more easily outcompete NOB during the aerated periods. Also, with intermittent aeration the energy demand is lowered.

To keep the DO at the desired level, the aeration can be controlled with a PID controller using feedback from measurements of the DO - see the following section.

2.6 PID controller

A PID controller is an algorithm containing a proportional, an integral, and a derivative part for calculating a controlling input signal, $u(t)$, to a system. It is used to keep a certain process variable as close as possible to a set reference value, $r(t)$. The controller also needs a measured feedback value, $y(t)$, from a sensor in the system. It aims to get the controlled process variable as close as possible to the reference value by minimizing the error value, $e(t)$; calculated as $e(t) = r(t) - y(t)$. In the same time, the error correction should be carried out in a 'smooth' way, i.e. without getting excessive deviations in the input signal. Mathematically the control algorithm for a PID controller can be formulated as:

$$u(t) = K_p e(t) + K_i \int e(t)dt + K_d \frac{de(t)}{dt}, \tag{2.6}$$

where K_p is the proportional coefficient, K_i is the integral coefficient, and K_d is the derivative coefficient.

In our case, the aeration flow is the controlling input signal, the DO is the controlled process variable, the measurement value from a DO sensor is the feedback value, and our desired DO level is used as the reference value. The reference value can be varied to obtain different values of the controlled process variable, as in the case with intermittent aeration. Furthermore, a controller can keep the controlled variable at a fairly stable level even when disturbances alter the conditions for the system, such as when variations in the influent flow change the composition of the bulk liquid in a biological wastewater treatment tank.

Chapter 3

Modelling of the biological system

In this chapter the mathematical modelling approach of the anammox process with MBBR, described in the previous chapter, is outlined. The developed model can be used on its own to study the process itself, or be implemented together with models of other wastewater treatment processes to study the interactions between them, or to study the performance of an entire wastewater treatment plant.

3.1 Modelling of biological wastewater treatment processes

The processes in a biological reactor can be divided into two essential types: conversion processes and transport processes. The biological and chemical conversion processes are independent of the type and of the size of reactor etc.; they only depend on the concentrations at the location where the reaction takes place. Physical transport processes on the other hand, for example mixing, aeration, and flow, depend on the specific implementation; they determine the local concentrations that the conversion processes are dependent on.

When modelling a biological system, a conceptual basis which identifies the physical, biological, and chemical mechanisms governing the system has to be formulated first. A model does not have to include every reaction in the system to be described; it is enough that it describes the part of interest in an accurate way. Since the wastewater treatment process is highly non-linear, and thus cannot be described satisfactory by linear equations, a good model cannot be obtained empirically. Instead, the relevant compounds and processes have to be identified in order to be able to translate them into process rates and stoichiometric interactions - that will form the basis of the model.

There are mainly two types of mathematical models with regard to time: steady state models, and dynamic models. A steady state model has constant loads and flows, it is thus not time-dependent. A dynamic model is more complex and has time-varying loads and flows, it is therefore dependent upon time. Which type of model to use depends on the purpose; steady state models are useful in design processes where all the system parameter might not be known, whereas dynamic models can help predicting the behavior of a proposed or already existing model. (Henze 2008)

3.2 Activated Sludge Models (ASM)

The most well known and most commonly used mathematical models for activated sludge processes are the Activated Sludge Models (ASM) by the International Water Association (IWA). The first version, Activated Sludge Model No.1 (ASM1), (Henze et al. 1987), was published in 1987. It had the ability to
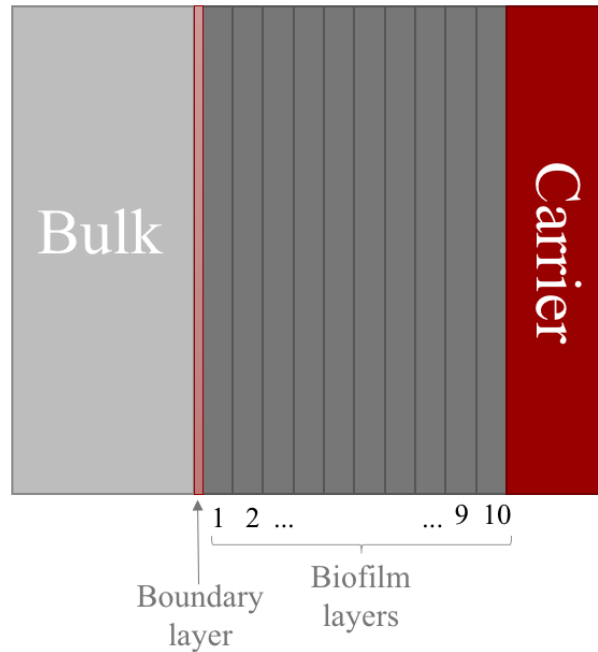
Figure 3.1: Sketch of the biofilm model

dynamically simulate the degradation of organic matter and the nitrification/denitrification processes. In ASM2 (Henze et al. 1995), presented 1995, newly acquired knowledge about the phosphorus removal was included. ASM2 was extended in 1999 with denitrifying phosphorus-accumulating organisms, called ASM2d (Henze et al. 1999). The latest model, ASM3 (Gujer et al. 1999), was proposed in 1999 and is a further development of ASM1 and ASM2.

In ASM1, ASM2, and ASM2d the sludge is split up into fractions; inert organic matter, nitrifying bacteria, denitrifying bacteria, heterotrophic bacteria and phosphate removing bacteria. In ASM3 the metabolism of the bacteria and the metabolic route inside them was included, giving a more complex model. Even though ASM3 is more detailed, the one significant improvement is the reliability of the output quality of the phosphorus. (Henze 2008)

The ASM can be considered state-of-the-art and is used in many platforms modelling wastewater treatment plants. It is made up of a set of differential equations describing the dynamics of the state variables. As an activated sludge model is describing a conversion process, it is independent of the type and the size of the reactor; it describes biological and chemical processes only through process rates and stoichiometric parameters. Therefore, the ASM can be developed and applied to different types of reactors. Physical transport models can then be applied for a specific plant, such as volume, aeration etc.. An ASM can be coupled together with models for other processes used in wastewater treatment plants to simulate interactions between different processes, and also to make a complete model of an entire wastewater plant.

3.3   Biofilm modelling

To model the MBBR, a biofilm model must be implemented. The model used in Lindblom's model (Lindblom et al. 2015), influenced by the model used in the WEST 3.7.3 - a simulation software for dynamic modelling and simulation of wastewater treatment plants, will be outlined in this section along with theory generally applicable to biofilm modelling.

The biofilm model was modelled one-dimensional with bulk and ten biofilm layers, as sketched in Figure 3.1. All the layers and the bulk are assumed to be completely mixed. The biofilm/bulk-interactions, the diffusion of substrates between the layers, and the consumption/production within the layers are all included in the model.

In the model, the soluble components in the bulk liquid diffuses into the biofilm through a thin, liquid membrane with thickness L_0 [m]. The particulate components in the bulk liquid interacts with the biofilm through an attachment/detachment process with the outermost layer. In the biofilm, the soluble components diffuses between the layers with different diffusion coefficients for the different components. Particulates are modelled to diffuse between the layers with a common low diffusion coefficient, D_X [md^{-1}]. The modelling results in a set of differential mass balance equations: one for the bulk liquid, one for the outermost layer - layer 1, one for layer 2-9, and one for the innermost layer - layer 10; these can be implemented in a suitable software, such as for example Matlab.

3.3.1 Diffusion

The molecular diffusion, the substrate utilization, and the accumulation of substrates within the biofilm are, in the continuous case, related by a set of second order partial differential equations on the form

$$\frac{\partial S}{\partial t} = D\frac{\partial^2 S}{\partial x^2} - r, \tag{3.1}$$

where the term on the left hand side describes the accumulation; the first term on the right hand side describes the diffusion; the last term on the right hand side describes the reaction. The variable S [g/m^3] is the substrate concentration in the biofilm, x [m] is the distance from the surface of the biofilm, t [d] is the time, D [m^2/d] is the diffusion coefficient in the biofilm, and r [g/m^{3}d] is the rate of substrate conversion per biofilm volume as in equation 3.4. The two boundary conditions necessary to solve equation 3.1 are: 1) $\frac{dS}{dx} = 0$ closest to the carrier, and 2) $S = S_L$ outermost in the biofilm, where S_L is the outermost substrate concentration in the biofilm. Since no analytic solution can be found for these equations, numerical methods have to be used in order to solve them.

The substrate flux, J [g/(m^{2}d)], in the biofilm is proportional to the gradient of the concentration and thus given by (Henze 2008):

$$J(x) = -D\frac{dS(x)}{dx} \tag{3.2}$$

3.3.2 Stoichiometry and kinetic process rates

Stoichiometry is based on mass balance equations and describes the relation between the reactants and the products in a chemical reaction in a quantitative manner. The stoichiometric relations of a process can be described in an orderly manner in a stoichiometric matrix, see for example Table 3.4. Each reaction described in the stoichiometric matrix has a corresponding process rate. The conversion rate of each compound is found by multiplying the yield coefficient in the stoichiometric matrix with the corresponding rate. Following ASM, the rate equation, describing the rate of the substrate utilization, follows Monod kinetics. Using Monod kinetics, the growth rates, μ [d^{-1}], of the microorganisms are on the form

$$\mu = \mu_{max}\frac{S}{K_S + S}, \tag{3.3}$$

where μ_{max} [d^{-1}] is the maximum growth rate, K_S [g/m^3] is the Monod half-saturation coefficient, and S [g/m^3] is the limiting substrate concentration.

In general, when growth, decay and other such reactions are involved, the mass balance of the state component S_i [g/m^3] (the rate r) is expressed as:

$$r = dS_i/dt = Q(S_{in} - S_i)/V + \sum_{j=1...N} \rho_j \nu_{i,j}, \qquad (3.4)$$

where S_{in} is the inflow of the component, Q [m^3/d] is the volumetric flow rate (the integration of the flux, $J(x)$, over an area), and V [m^3] is the volume. The term $\sum_{j=1...N} \rho_j \nu_{i,j}$ is the sum of the kinetic rates, ρ_j, for process j multiplied by the yield coefficient $\nu_{i,j}$ from the stoichiometric matrix for process j and state component i, and N is the total number of process rates.

3.3.3 Biofilm thickness

Within the layers, reactions occur according to the stoichiometric matrix in Table 3.4. The thicknesses of the layers are then recalculated in every iteration. Mass is assumed to fall off from the biofilm and migrate into the bulk liquid if the sum of the thicknesses exceed a predefined maximum value.

The change of the thickness of the biofilm over time, $\frac{dL}{dt}$ [m/d], can be calculated as

$$\frac{dL}{dt} = u(L) - u_{Att} - u_{Det}, \qquad (3.5)$$

where u [m/d] describes the net effect of growth and decay processes within the biofilm; L [m] is the thickness of the biofilm; u_{Att} [m/d] describes the surface attachment velocity; u_{Det} [m/d] describes the surface detachment velocity. u_{Det} is in this case described by

$$u_{Det} = k_{Det}L^2, \qquad (3.6)$$

where k_{Det} [1/(d $\cdot$ m)] is the detachment rate coefficient. (Henze 2008)

3.4 Lindblom's model

The model used in this project is created by Erik Lindblom at Stockholm Vatten; described and used in (Lindblom et al. 2015) and also used in (Lindblom et al. 2016). It is a dynamic model, describing the one-stage anammox process with MBBR in side-stream processes, and including the production of nitrous oxide. It is based on the Activated Sludge Model for Nitrogen (ASMN) (Hiatt and Grady 2008), which in turn is based on the Activated Sludge Model No.1 (ASM1). In the nitrification/denitrification process AOB conversion is the rate limiting reaction since nitrite is converted to nitrate almost immediately. Therefore, it is often modeled as one process where the AOB convert ammonium directly to nitrate. That is also the case in the ASMs. In addition, the ASMs is designed for modelling of processes at temperatures of 5-20 °C, at which almost no nitrite accumulation takes place (Henze 2008). As a consequence, nitrite is not included in the ASMs. In order to be able to include the anammox process, which utilizes nitrite, a modification has to be done: nitrification in two steps instead of one. That is done in ASMN, and that model was subsequently included in Lindblom's model. Another reason for including nitrite in the model was that one of Lindblom's aims was to include production routes of nitrous oxide, where nitrite plays an important role (Lindblom et al. 2015).

Furthermore, the principles for autotrophic denitrification was implemented in accordance with (Mampaey et al. 2013), scenario A. An additional component, X_AMX, for anammox biomass was also introduced in agreement with the model proposed in (Hao et al. 2002). This model implies that when the oxygen level is almost zero, X_AMX converts NO_2^- and NH_4^+ mainly to N_2 during growth, but also

11

NO_3^- (Lindblom et al. 2015). In addition, a model for stripping of nitrous oxide was implemented in accordance with (Foley et al. 2015).

The reactions in the bulk are modelled conventionally as in ASM and the biofilm is modelled using the biofilm model described in section 3.3.

The components used in this model are listed, along with description and unit, in Table 3.1. The input concentrations of these components can been seen in Table 3.2. The parameter values used in this model are listed in Table 3.3. Parameters mentioned in (Lindblom et al. 2015) but not used in the simulation are left out. Also, $KI10FNA$, not in (Lindblom et al. 2015) but used in the model, is added. The stoichiometric matrix, describing the stoichiometric relations in the model can be seen in Table 3.4. The process rates associated with the stoichiometric matrix in Table 3.4 are listed in Table 3.5.

Comp.	Unit	Description
S_I	gCOD/m^3	Inert soluble organic matter
S_S	gCOD/m^3	Readily biodegradable substrate
X_I	gCOD/m^3	Inert particulate organic matter
X_S	gCOD/m^3	Slowly biodegradable substrate
X_H	gCOD/m^3	Active heterotrophic biomass
X_{AOB}	gCOD/m^3	Active AOB biomass
X_P	gCOD/m^3	Particulate produced from biomass decay
S_O	gCOD/m^3	Dissolved oxygen
S_{NO3}	gN/m^3	Nitrate
S_{NH4}	gN/m^3	Ammonia
S_{ND}	gN/m^3	Soluble biodegradable organic nitrogen
X_{ND}	gN/m^3	Particulate biodegradable organic nitrogen
S_{ALK}	molar units	Alkalinity
X_{TSS}	gCOD/m^3	Total suspended solids
S_{NO2}	gN/m^3	Nitrite
S_{NO}	gN/m^3	Nitric oxide
S_{N2O}	gN/m^3	Nitrous oxide
S_{N2}	gN/m^3	Nitrogen
X_{NOB}	gCOD/m^3	Active NOB biomass
X_{AMX}	gCOD/m^3	Active AMX biomass

Table 3.1: Components in Lindblom's model

Comp.	Conc.	Unit
S_I	280	gCOD/m³
S_S	76	gCOD/m³
X_I	200	gCOD/m³
X_S	110	gCOD/m³
X_H	0	gCOD/m³
X_{AOB}	0	gCOD/m³
X_P	0	gCOD/m³
S_O	0	gCOD/m³
S_{NO3}	0	gN/m³
S_{NH4}	769	gN/m³
S_{ND}	19	gN/m³
X_{ND}	16	gN/m³
S_{ALK}	35	molar units
X_{TSS}	232.5	gCOD/m³
S_{NO2}	0.0907	gN/m³
S_{NO}	25	gN/m³
S_{N2O}	0	gN/m³
S_{N2}	0	gN/m³
X_{NOB}	0	gCOD/m³
X_{AMX}	0	gCOD/m³

Table 3.2: Input concentrations to the system

Symbol	Value	Unit	Definition
f_P	0.08	-	Fraction of biomass leading to particulate products
i_{XB}	0.086	g N/(g cell COD)	Mass of N per mass of COD in biomass
i_{XP}	0.06	g N/(g COD)	Mass of N per mass of COD in products from biomass
Heterotrophic bacteria			
η_H	6.0	d^{-1}	Maximum specific growth rate
b_H	0.4	d^{-1}	Decay rate coefficient
k_a	0.04	m³/(g COD d)	Ammonification rate coefficient
k_h	2.208	g COD/(g cell COD d)	Hydrolysis rate coefficient
K_X	0.15	g COD/(g cell COD)	Half-saturation coefficient for hydrolysis of slowly biodegradable substrate
$\eta_{max,H}$	0.4	-	Anoxic hydrolysis factor
Y_H	0.6	g cellCOD/(g COD)	Heterotrophic yield
η_g	0.9	-	Anoxic yield factor
η_{g2}	0.28	-	Anoxic growth factor
η_{g3}	0.16	-	Anoxic growth factor
η_{g4}	0.35	-	Anoxic growth factor
η_{g5}	0.35	-	Anoxic growth factor
K_{S1-4}	20	g COD/m³	Half-saturation coefficient for substrate
K_{S5}	38	g COD/m³	Half-saturation coefficient for substrate
$K_{O,H1-5}$	0.1	g O₂/m³	Half-saturation coefficient, O₂
K_{NO3}	0.2	g N/m³	Half-saturation coefficient, NO₃
K_{NO2}	0.2	g N/m³	Half-saturation coefficient, NO₂
K_{NO}	0.05	g N/m³	Half-saturation coefficient, NO
K_{N2O}	0.05	g N/m³	Half-saturation coefficient, N₂O
K_{I3NO}	0.5	g N/m³	Inhibition coefficient, NO

Symbol	Value	Unit	Definition
K_{I4NO}	0.3	g N/m^3	Inhibition coefficient, NO
$K_{I5FNA,HET}$	10	g N/m^3	Parameter for limitation of FNA
AOB bacteria			
η_{A1}	1.4127	d^{-1}	Maximum specific growth rate
b_{A1}	0.08	d^{-1}	Decay rate coefficient
Y_{A1}	0.18	g cell COD/(g N)	Autotrophic yield
K_{OA1}	1.0	g O$_2$/m^3	Half-saturation coefficient, O$_2$
K_{FA}	0.0525	g N/m^3	Half-saturation coefficient for FA, autotrophic growth
K_{I9FA}	1.0	g N/m^3	FA inhibition coefficient
K_{I9FNA}	0.1	g N/m^3	FNA inhibition coefficient
$K_{FA,AD}$	1e3	g N/m^3	Half-saturation coefficient for FA, denitrification
$K_{FNA,AOB}$	1e-3	g N/m^3	Half-saturation coefficient, HNO$_2$
$f_{DNT,A}$	0.0025	-	Fraction of NH$_3$ oxidized with NO$_2$ as partial electron acceptor (scenario A)
$K_{NO,AOB}$	0.06	g N/m^3	Half-saturation coefficient, NO
NOB bacteria			
η_{A2}	1.0761	d^{-1}	Maximum specific growth rate
b_{A2}	0.0494	d^{-1}	Decay rate coefficient
Y_{A2}	0.06	g cell COD/(g N)	Autotrophic yield
K_{OA2}	1.8	g O$_2$/m^3	Half-saturation coefficient, O$_2$
K_{FNA}	1e-4	g N/m^3	Half-saturation coefficient for FNA, HNO$_2$
$KI10FA$	1000	g N/m^3	FA inhibition coefficient
$KI10FNA$	400	g N/m^3	FNA inhibition coefficient
Anammox bacteria			
η_{AMX}	0.0447	d^{-1}	Maximum specific growth rate
b_{AMX}	0.0027	d^{-1}	Decay rate coefficient
Y_{AMX}	0.159	g cell COD/(g N)	Anammox yield, as in (Hao et al. 2002)
$K_{O_2,AMX}$	0.01	g O$_2$/m^3	Half-saturation coefficient, O$_2$
$K_{NH,AMX}$	0.14	g N/m^3	Half-saturation coefficient, NH$_4$
$K_{NO_2,AMX}$	1	g N/m^3	Half-saturation coefficient, NO$_2$
Stripping			
D_{O_2}	2.12e-9	m^2/s	Diffusion coefficient, O$_2$
D_{N_2O}	1.77e-9	m^2/s	Diffusion coefficient, N$_2$O
D_{N_2}	1.86e-9	m^2/s	Diffusion coefficient, N$_2$
D_{NO}	8.7e-11	m^2/s	Diffusion coefficient, NO
Biofilm			
L_{max}	1.2	mm	Maximum biofilm thickness
L_0	56	μm	Boundary layer thickness
ρ	5e4	g TS /m^3	Biofilm density
η	0.5	-	Porosity of the biofilm
k_{Att}	0.1	1/(d $\cdot$ m)	Attachment rate of particulates
k_{Det}	1e5	1/(d $\cdot$ m)	Biofilm detachment rate
D_X	5e-14	m^2/s	Diffusion in biofilm coefficient particulate components
D_{SI}	6.9e-10	m^2/s	Diffusion coefficient biofilm, inert soluble COD
D_{SS}	1.2e-9	m^2/s	Diffusion coefficient biofilm, soluble COD
D_{O_2}	2.2e-4	m^2/s	Diffusion coefficient biofilm, O$_2$

Symbol	Value	Unit	Definition
D_{NO_3}	1.6e-9	m^2/s	Diffusion coefficient biofilm, NO$_3$
D_{NH_4}	1.74e-9	m^2/s	Diffusion coefficient biofilm, NH$_4$
D_{SND}	1.37e-9	m^2/s	Diffusion coefficient biofilm, soluble organic N
D_{NO_2}	1.28e-9	m^2/s	Diffusion coefficient biofilm, NO$_2$
D_{NO}	8.7e-11	m^2/s	Diffusion coefficient biofilm, NO
D_{N_2O}	1.77e-9	m^2/s	Diffusion coefficient biofilm, N$_2$O
D_{N_2}	1.86e-9	m^2/s	Diffusion coefficient biofilm, N$_2$

Table 3.3: Parameter values used in Lindblom's model

	S_S	X_S	X_H	X_{AOB}	X_P	S_O	S_{NO3}	S_{NH4}	S_{ND}	X_{ND}	S_{NO2}	S_{NO}	S_{N2O}	S_{N2}	X_{NOB}	X_{AMX}
proc1	$-1/Y_H$		1			$-\frac{1-Y_H}{Y_H}$		$-i_{XB}$								
proc2x1	$-\frac{1}{Y_H*\eta_g}$		1				$-\frac{1-Y_H*\eta_g}{1.14385714*Y_H*\eta_g}$	$-i_{XB}$			$\frac{1-Y_H*\eta_g}{1.14385714*Y_H*\eta_g}$					
proc2x2	$-\frac{1}{Y_H*\eta_g}$		1					$-i_{XB}$			$-\frac{1-Y_H*\eta_g}{0.5714285*Y_H*\eta_g}$	$\frac{1-Y_H*\eta_g}{0.5714285*Y_H*\eta_g}$				
proc2x3	$-\frac{1}{Y_H*\eta_g}$		1					$-i_{XB}$				$-\frac{1-Y_H*\eta_g}{0.5714285*Y_H*\eta_g}$	$\frac{1-Y_H*\eta_g}{0.5714285*Y_H*\eta_g}$			
proc2x4	$-\frac{1}{Y_H*\eta_g}$		1					$-i_{XB}$					$-\frac{1-Y_H*\eta_g}{0.5714285*Y_H*\eta_g}$	$\frac{1-Y_H*\eta_g}{0.5714285*Y_H*\eta_g}$		
proc3x1				1		$-\frac{3.4285714-Y_{A1}}{Y_{A1}}$		$-i_{XB}-\frac{1}{Y_{A1}}$			$1/Y_{A1}$					
proc3x2						$-\frac{1.1428571-Y_{A2}}{Y_{A2}}$	$1/Y_{A2}$	$-i_{XB}$			$-1/Y_{A2}$				1	
proc4		$1-f_P$	-1		f_P					$i_{XB}-f_P*i_{XP}$						
proc5x1		$1-f_P$		-1	f_P					$i_{XB}-f_P*i_{XP}$						
proc5x2		$1-f_P$			$2f_P$					$i_{XB}-f_P*i_{XP}$					-1	
proc6								1	-1							
proc7	1	-1														
proc8									1	-1						
proc9A				1		$-\frac{2.29-Y_{A1}}{Y_{A1}}$		$-i_{XB}-\frac{1}{Y_{A1}}$			$-1/Y_{A1}$	$2/Y_{A1}$				
proc10A				1		$-\frac{2.29-Y_{A1}}{Y_{A1}}$		$-i_{XB}-\frac{1}{Y_{A1}}$			$1/Y_{A1}$	$-2/Y_{A1}$	$2/Y_{A1}$			
proc11							$1/1.14$	$-i_{XB}-\frac{1}{Y_{AMX}}$			$-\frac{1}{Y_{AMX}}-\frac{1}{1.14}$			$2/Y_{AMX}$		1
proc12		$1-f_P$								$i_{XB}-f_P*i_{XP}$						-1

Table 3.4: Stoichiometric matrix, yield coefficients for all ...

Table 3.5: Process rates

Process	Value	Description
proc1	$\mu_H * X_H * \left(\frac{S_S}{K_{S1}+S_S}\right) * \left(\frac{S_O}{K_{OH1}+S_O}\right)$	Aerobic growth of heterotrophs
proc2x1	$\mu_H * \eta_{g2} * X_H * \left(\frac{S_S}{K_{S2}+S_S}\right) * \left(\frac{S_{NO3}}{K_{NO3}+S_{NO3}}\right) * \left(\frac{K_{OH2}}{K_{OH2}+S_O}\right)$	Anoxic growth of heterotrophs, reducing nitrate to nitrite
proc2x2	$\mu_H * \eta_{g3} * X_H * \left(\frac{S_S}{K_{S3}+S_S}\right) * \left(\frac{S_{NO2}}{K_{NO2}+S_{NO2}}\right) * \left(\frac{K_{OH3}}{K_{OH3}+S_O}\right) * \left(\frac{K_{I3NO}}{K_{I3NO}+S_{NO}}\right)$	Anoxic growth of heterotrophs, reducing nitrite to nitric oxide
proc2x3	$\mu_H * \eta_{g4} * X_H * \left(\frac{S_S}{K_{S4}+S_S}\right) * \left(\frac{S_{NO}}{K_{NO}+S_{NO}+S_{NO}^2/K_{I4NO}}\right) * \left(\frac{K_{OH4}}{K_{OH4}+S_O}\right)$	Anoxic growth of heterotrophs, reducing nitric oxide to nitrous oxide
proc2x4	$\mu_H * \eta_{g5} * X_H * \left(\frac{S_S}{K_{S5}+S_S}\right) * \left(\frac{S_{N2O}}{K_{N2O}+S_{N2O}}\right) * \left(\frac{K_{OH5}}{K_{OH5}+S_O}\right) * \left(\frac{K_{I5,FNA,HET}}{K_{I5,FNA,HET}+S_{FNA}}\right)$	Anoxic growth of heterotrophs, reducing nitrous oxide to nitrogen, including FNA inhibition
proc3x1	$\mu_{A1} * X_{AOB} * \left(\frac{S_{FA}}{K_{FA}+S_{FA}+S_{FA}^2/K_{I9FA}}\right) * \left(\frac{S_O}{K_{OA1}+S_O}\right) * \left(\frac{K_{I9FNA}}{K_{I9FNA}+S_{FNA}}\right)$	Autotrophic growth of AOB
proc3x2	$\mu_{A2} * X_{NOB} * \left(\frac{S_{FNA}}{K_{FNA}+S_{FNA}+S_{FNA}^2/K_{I10FNA}}\right) * \left(\frac{S_O}{K_{OA2}+S_O}\right) * \left(\frac{K_{I10FA}}{K_{I10FA}+S_{FA}}\right)$	Autotrophic growth of NOB
proc4	$b_H * X_H$	Death and lysis of heterotrophs
proc5x1	$b_{A1} * X_{AOB}$	Death and lysis of AOB
proc5x2	$b_{A2} * X_{NOB}$	Death and lysis of NOB
proc6	$k_a * S_{ND} * X_H$	Ammonification
proc7	$k_h * X_H * \left[\left(\frac{X_S}{X_H}\right)/\left(K_X + \frac{X_S}{X_H}\right)\right] * \left[\left(\frac{S_O}{K_{OH1}+S_O}\right) + \eta_h * \left(\frac{K_{OH1}}{K_{OH1}+S_O}\right) * \left(\frac{S_{NOX}}{K_{NO3}+S_{NOX}}\right)\right]$	Hydrolysis of particulate organics
proc8	$proc7 * \left(\frac{X_{ND}}{X_S}\right)$	Hydrolysis of particulate organic nitrogen
proc9A	$f_{DNT_A} * \mu_{A1} * X_{AOB} * \left(\frac{S_{FA}}{K_{FA,AD}+S_{FA}}\right) * \left(\frac{S_O}{K_{OA1}+S_O}\right) * \left(\frac{S_{FNA}}{K_{FNA,AOB}+S_{FNA}}\right)$	AOB denitrification 1, NH4+O2+NO2 => NO
proc10A	$\mu_{A1} * X_{AOB} * \left(\frac{S_{FA}}{K_{FA,AD}+S_{FA}}\right) * \left(\frac{S_O}{K_{OA1}+S_O}\right) * \left(\frac{S_{NO}}{K_{NO,AOB}+S_{NO}}\right)$	AOB denitrification 2, NH4+02+NO => N2O
proc11	$\mu_{AMX} * X_{AMX} * \left(\frac{S_{NH4}}{S_{NH4}+K_{NH,AMX}}\right) * \left(\frac{S_{NO2,AMX}}{S_{NO2}+K_{NO2,AMX}}\right) * \left(\frac{K_{O2,AMX}}{K_{O2,AMX}+S_O}\right)$	Anammox process
proc12	$b_{AMX} * X_{AMX}$	Anammox process

3.4.1 Inputs

The pH and temperature are assumed to be constant at 7.1 and 25⁰C respectively. The concentration of compounds in the input flow are assumed to be constant. For the aeration, the gas exchange of oxygen, KLa $[d^{-1}]$, is used as an the input in order to control the concentration of DO in the bulk. Intermittent aeration with 45 minutes of aeration is followed by 15 minutes of mixing with the aeration turned off. This is modelled with a PID-regulator, controlling the value of $K_L a$ to obtain a value of DO of 1.5 g O_2/m^3 during the aerobic period and a value of DO of 0 g O_2/m^3 during the anoxic period. The rest of the inputs to the system are listed in Table 3.2.

Chapter 4

Method

4.1 Implementation

The model by Lindblom (Lindblom et al. 2015) was implemented and evaluated in the software Matlab/Simulink 2016a; the code for the evaluation is enclosed in appendix A. Screen-shots of the Simulink model can be seen in Figure 4.1 and Figure 4.2.
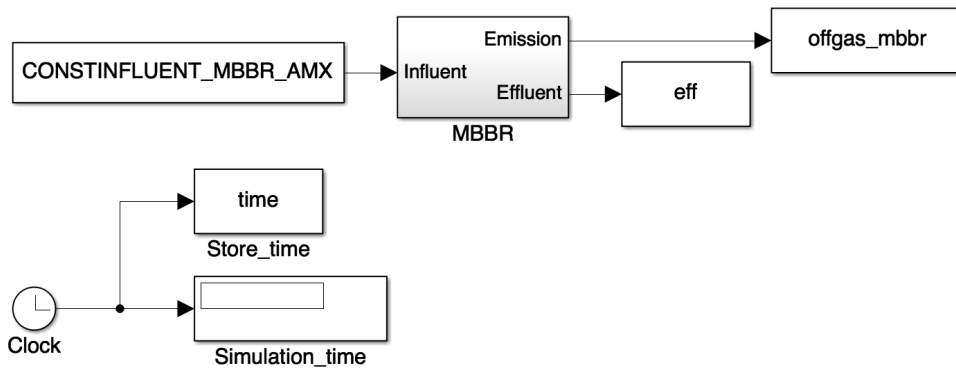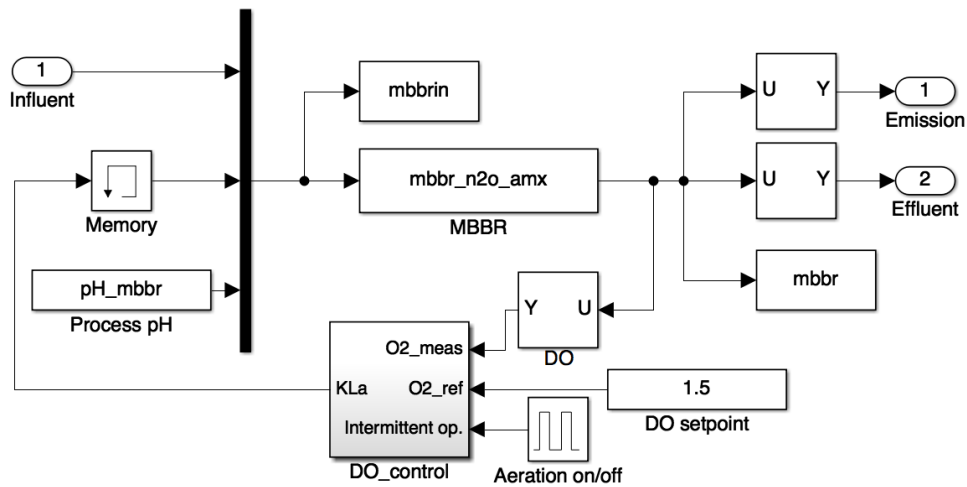

Figure 4.1: Simulink 1

Figure 4.2: Simulink model of the MBBR

In Figure 4.1 the Simulink model of the input to, and output from, the MBBR is shown along with the time used. In Figure 4.2 the Simulink model of the MBBR can be seen. The differential equations described in section 3.3 were implemented as an S-function written in C, called mbbr_n2o_amx. In Matlab, this is compiled with the command `mex`. The DO control was implemented as an user-defined PID controller, called DO_control, with its measured feedback value, DO, taken from the output of mbbr_n2o_amx; its reference value was taken from a set constant value, which is used when the aeration is on, together with a step function turning the aeration on and of; its output value, $K_L a$, as input to mbbr_n2o_amx. The constant pH-value was implemented as an input parameter to mbbr_n2o_amx. Influent, emission and effluent are also connected to the model.

For solving the differential equations, the Matlab solver ode45 (Dormand-Prince) was used, which uses variable step size, since it was found to give the shortest run time with maintained accuracy. The sample times at which to save the states of the system were explicitly specified. The full simulation runs for 53 days, after which the outputs of the model can be fetched. The outputs show the states of the system during the whole simulation for: MBBR states, effluent, off-gas emissions, input values, time vector, DO level, and controller states.

4.2   Optimizations

When starting to run the model, one simulation on my personal computer took about 20 minuter and almost 50 minutes on the cluster (see section 4.5.1). Since the model would be used many times for different tests and has to be run thousands of times in the calibration, possible reduction of the simulation time would greatly facilitate further work. Therefore, effort was made at optimizing the execution of the simulation. The optimizations made will be described in the following subsections. The modifications made resulted together in reducing the simulation time to approximately 1/5 of the original time - a substantial improvement.

4.2.1   Parallelization

Some changes had to be made in order to enable the simulations to run in parallel with one another on the cluster computers, see section 4.5.1. Matlab's Parallel Computing Toolbox, including `parfor`, was used to enable Matlab's parallel computing abilities. Within the `parfor`-loop, the inputs to the Simulink model have to be explicitly assigned to the model workspace instead of loaded only into the base workspace. This is done with the Matlab function `assagnin`. When the job is submitted to the cluster, the number of cores to be used has to be specified. Matlab's Distributed Computer Server, available on the cluster computers, then uses a job scheduler to coordinate the workers performing the parallelized job - one worker per core.
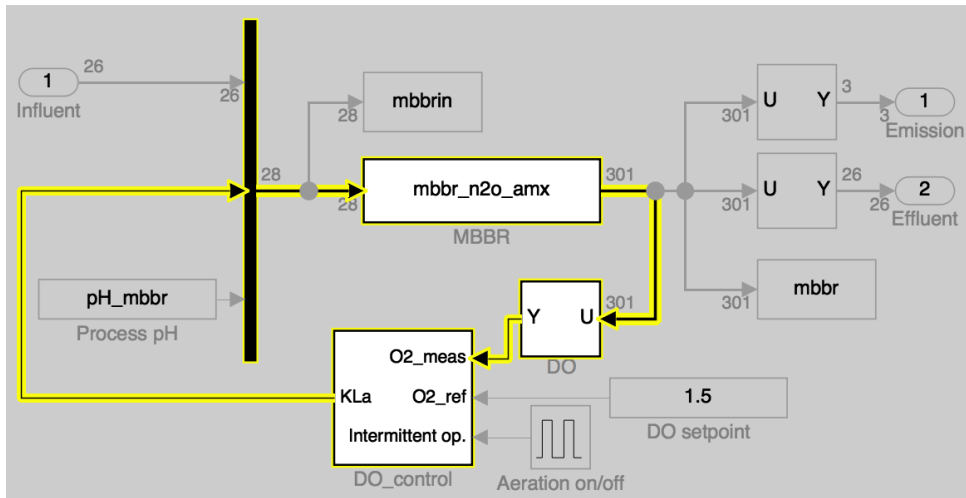
4.2.2 Algebraic loops

Figure 4.3: Algebraic loop in the Simulink model

Algebraic loops arise when an output of a block with direct feedthrough drives an input port to the same block, either directly or through other blocks also having direct feedthrough. In our case, this is what happens when using the PID-controller with direct feedback, see Figure 4.3. Matlab has a built-in function that can detect and often solve the algebraic loop. However, this can make the model run slower since Matlab has to solve the algebraic loop iteratively in every time step. Therefore, the algebraic loop was eliminated manually by inserting a continuous memory block in the feedback path, as can be seen in Figure 4.2. The memory block applies a one integration step delay, meaning that the output is the previous input value. This insertion breaks the direct feedthrough of the feedback path, consequently eliminating the algebraic loop.

4.2.3 Simulation modes

Simulink offers three simulation modes: normal, accelerated, and rapid accelerated mode. The accelerated modes offer faster runs at the expense of trade offs - like longer build times, and stricter requirements. For example, no algebraic loops shall be present for rapid acceleration mode, all code in the Simulink blocks must be available as C code, and the full model must be capable of generating code.

4.2.4 Build optimizations

For the compilation with gcc of the C-code for the S-function, optimizations for speed is done with the flag '-O3', enabling almost all the gcc optimizations for faster execution speed. With -O3, code size, compilation time, and debugging possibilities are trade off against execution speed. Also, all CPU instructions on the hardware is enabled with the flag '-march=native'. Furthermore, some of the Simulink optimizations were turned on in order to optimize for execution speed. Some of optimizations done in Simulink were: 1) Enable inlining of parameters, 2) increased loop unrolling threshold, 3) compiler optimizations on for faster runs, 4) the 'ensure responsiveness' option turned off, 5) the build configurations set to 'faster runs', and 6) the 'prioritized objectives' set to 'execution efficiency'. Also, when the code was proven to be working, as much of Matlab's error checking as possible were turned off since some of them are run-time checks that slow down the execution. The trade offs for these optimizations were the

same as those for the C-code, plus reduced interactivity of the model. An improvement, not implicating a trade off, is that the hardware used can be specified in Simulink, ensuring that the resources are used in the most efficient way.

4.3   Reproduction of results

The code for the model was originally provided without consulting Lindblom for specifics. Since the code did not function properly, the first step in the research process was to reproduce the given model; the plots of MBBR anammox, see figure 3 in (Lindblom et al. 2016), were reproduced in order to verify that the given model is used correctly. After contacting Lindblom personally, it turned out that a part of the code, that had not yet been sufficiently verified yet, had to be turned off in order to make the simulations run. Also, the original initial values and the code for the PID-controller used had to be requested from Lindblom personally.

4.4   Sensitivity analysis

A sensitivity analysis can be performed to identify the parameters most sensitive to uncertainties. These parameters are the ones that will be considered later in the calibration of the model. The calibration was done on all model parameters, seen in Table 3.3, except for the diffusion coefficients for the stripping model. These values can be seen as "exactly" known and will thus not vary.

There are several methods for doing a sensitivity analysis. Since the model is highly complex and each simulation takes about 5 minutes to run on a desktop computer (4 GB RAM, 1.8 GHz), the simplest method, one-at-a-time (OAT), has been chosen. OAT has a computational expense of $O(N)$, where N is the number of parameters examined. With OAT, one parameter at a time is changed from its nominal value and the effect on the output of the simulation is then quantified. Before continuing with the next parameter the value of the tested parameter is returned to its original value. OAT does not fully explore the input space, i.e. the effect of simultaneous variations is neglected. For that to be examined, other methods, such as a variance-based sensitivity analysis, have to be used with a computational expense of $O(N^2)$.

OAT tells us the impact of each individual parameter in each of the outputs. It subsequently answers the question: How does an uncertainty of each of the inputs contribute to the uncertainty of each of the outputs? Thus, after performing a sensitivity analysis we know which parameters to focus on in the calibration in order to increase the correctness of the model. OAT also gives us a relation between the inputs and the outputs of the model that is hard to derive due to the complexity of the model.

The sensitivity analysis tells us which of the input parameters is most sensitive to uncertainties. This information can be used to reduce the number of parameters varied in the calibration of the model. This is of considerable importance since the calibration has the computational complexity $O(N^2)$, where N is the number of parameters to be varied.

The model reaches a periodic steady state within 53 days. Therefor, in order to save time, the outputs after 55 days can be assumed to be approximately the same as after 53 days. Using this assumption, the states of the MBBR and the PID controller after 53 days can be saved and used as initial values for new simulations simulated for 2 days. The outputs of the last hour of the 2 days of simulation with unperturbed parameter space were compared with the outputs of the last hour of the 2 days of simulations with perturbed parameter spaces. Using this construction, each simulation with a new parameter set only has to be run for 2 days instead of 53 days.

The sensitivity coefficient, $\sigma_y^{\Delta p}$, is a quantitative measure of how much an output has been changed, in percentage, due to a new set of parameter values compared to the nominal parameter values. It is calculated as

$$\sigma_y^{\Delta p} = \frac{1}{T_S} \int_0^{T_S} \frac{y(p + \Delta p, t) - y(p, t)}{y(p, t)} dt, \tag{4.1}$$

where Δp is the perturbation, T_S the length of the compared time interval, y the output, p the nominal parameter value, and t the time variable. The expression

$$\frac{1}{b - a} \int_a^b f(x) dx \tag{4.2}$$

in continuous time corresponds to mean($f(x)$) in discrete time. Thus, the sensitivity coefficient in discrete time is calculated as

$$\sigma_y^{\Delta p} = \text{mean} \left(\frac{y(p + \Delta p, t) - y(p, t)}{y(p, t)} \right). \tag{4.3}$$

The results of the simulation of 2 days with the nominal values of the parameters, as in Table 3.3, were saved: called 'the reference output'. The results from the simulations with the perturbed parameter sets were then evaluated against the reference output during the last hour of the simulation.

4.5 Calibration

The uncertainty in the most sensitive parameters, obtained from the sensitivity analysis, was assumed to be a normal distribution with an uncertainty range of $\pm 50\%$ from the nominal values in Table 3.3. Latin hypercube sampling (LHS) was used for the generation of new parameter sets. LHS was chosen over regular Monte Carlo-sampling to get a more even coverage of the possible combinations of parameter values than what a random sampling would have provided. This can be done in MATLAB with a function called `lhsdesign`, defining all the variations that will be used in a matrix.

The outputs that were evaluated were NH_4^+ in the effluent, N_2O in the off-gas, and N_2O in the effluent, since these were the only outputs with measurements available. 3000 simulations were run with the combinations obtained from LHS. The results from the simulation with the generated parameter values were evaluated against the experimental values in the same time interval as in Figure 5.1. The degree of fit between the model with the generated parameter values and the measurements for each of the evaluated outputs was calculated as

$$\text{FIT} = 1 - \frac{\text{norm}(y - \hat{y})}{\text{norm}(y - \text{mean}(y))} \tag{4.4}$$

where y is the experimental values and $\hat{y}$ is the simulated values. The value of FIT ranges between -inf and 1, where 1 indicates that the simulated values match the experimental values exactly; the Matlab function `godnessOfFit(ŷ,y,'NRMSE')`, where NRMSE stands for normalized root-mean-square error, executes precisely this and was subsequently used. The total FIT, FIT_{tot}, was calculated as the sum of the three individual FITs, implicating that the maximum total FIT would be 3:

$$\text{FIT}_{tot} = \text{FIT}_{NH_4^+, eff} + \text{FIT}_{N_2O, gas} + \text{FIT}_{N_2O, eff} \tag{4.5}$$

The results were fetched when the 3000 simulations with different parameter values for the five most sensitive parameters had been run on the cluster. The maximum value of the total FIT was found along with the corresponding position in the matrix. At the corresponding position in the LHS-matrix, the variations of the parameters was fetched and used to re-calculate the values of the parameters that had been found to give the maximum total FIT. A full simulation with the new parameter set was run and the output fetched.

4.5.1   Run on cluster

Since running 3000 simulations, each running for about 5 minutes, would take more than one week on my personal laptop, the calculations were run on cluster computers. The cluster provided was Tintin, a high performance computer cluster at UPPMAX. In the cluster, the cores are gathered in nodes, mostly containing 16 cores each. The simplest way to run the simulations in parallel on the cluster was to divide the runs into fractions, one for each node to run on. On each node 15 simulations can be run in parallel, since one core has to be used for the job scheduler that coordinates the workers on the rest of the cores. The code uploaded to the cluster builds the rapid accelerator target for model, runs the simulations in parallel and saves the calculated FIT-values for each of them.

After some test runs, 1 simulation on 1 core on the cluster was determined to take about 9 minutes. With the possibility to run 15 simulations in parallel per node that means that $15 * 60/9 = 100$ runs can be run per node and hour. When split the 3000 simulations onto 3 nodes, all simulations will be finished in reasonable 10 hours. With 3000 simulations to run and 5 parameters to vary, a 3000x5 matrix with the values of the variations of the 5 parameters was created with `lhsdesign` and then split up into 3 1000x5 matrices to be used on the 3 nodes. The rules of procedure in order to run the simulations on the cluster were as follows:

- Log in to the cluster account using ssh.

- Create folders for each node run, copy the code for the simulation to each of them.

- Load the module (program) Matlab and start it.

- Configure Matlab to run parallel jobs on the cluster by calling `configCluster`.

- Specify the parameters to be passed to the batch system - SLURM, with the jobs by editing `ClusterInfo`: specify the charge account (project name), set `WallTime`, and specify the partition to run on, here 'node' was used.

- Compile the S-function mbbr_n2o_amx.c with `mex` using gcc, share with all folders.

- Get a handle to the cluster with `c=parcluster`.

- Upload the job with `c.batch('name_of_code_nrX', 'pool', 15)` in each of the folders.

- Wait

- Fetch the outputs in Matlab, copy them to the local computer for concatenation and evaluation of the results.

Even though it is stated on the homepage of Matlab that the code working on my computer should work on cluster computers, it turned out to be the case that it needed some modifications in order to work. Different error messages appears with some generic error message (corrupted file, file does not exist, ascii does not match, unknown/not declared variable, etc) without any clue about what the true problem might be. The modifications that was proven to make the simulations working: Delete previous targets built; The initialized parameter values must be explicitly transferred from the base workspace to the model workspace, even outside the parfor-loop; The rapid accelerator target has to be build explicitly before starting the simulations.

Chapter 5

Results

5.1   Reproduction of results

In Figure 5.1 the result from the reproduction of the plots in figure 3 in (Lindblom et al. 2016) are shown. The results are quite similar to Lindblom's. However, the noticeable differences are that Lindblom's curves have small variations in figure D and H, whereas mine are smooth. In addition, my blue curve has an amplitude about 7 g N/m^3 lower than Lindblom's in figure F.
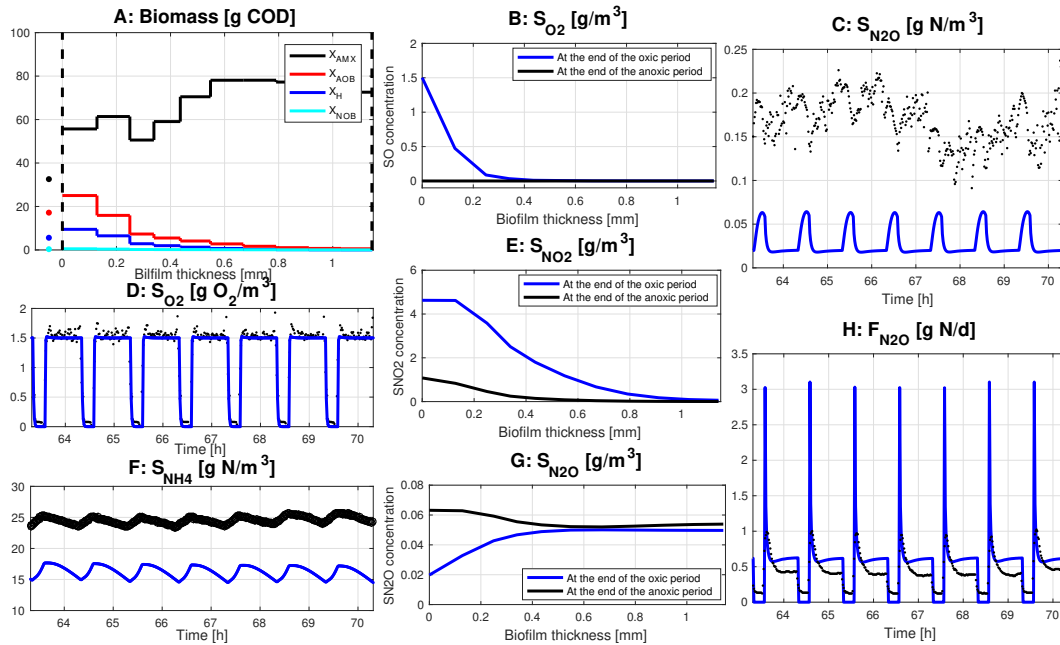
Figure 5.1: The reproduction of Lindblom's plots, as in figure 3 in (Lindblom et al. 2016); in figure A, the amount of simulated active biomass in the bulk (the dots on the extreme left) and the amount in the biofilm (the curves), are shown; in figure C, D, F, and H, the black dots show the measured values and the blue curves the simulation values of the amount of N$_2$O in the effluent, the amount of DO in the effluent, the amount of NH$_4$$^+$ in the effluent, and the amount of N$_2$O in the off-gas emission, respectively; in figure B, E, and G, the simulated concentrations of the DO in the biofilm, the NO$_2$ in the biofilm, and the N$_2$O in the biofilm, are shown as a function of the distance to the bulk. The blue lines show the concentrations at the end of the oxic period, and the black lines show the concentrations at the end of the anoxic period.

5.2 Sensitivity analysis

The results indicate that η, ρ, L_{max}, L_0, and Y_H are the five most sensitive parameters of the model, in decreasing order with respect to the sum of the absolute values of the obtained percentage changes in the outputs - plotted in Figure 5.2. Looking at the sensitivity summed over each of the outputs, see Figure 5.3, it is evident that there are significant differences in how much the outputs are affected when the parameter set used is changed. The sensitivity of all the parameter values, ordered as in Table 3.3, can be found in Figure 5.4. When these parameters are sorted ascending with respect to the calculated sensitivity, as in Figure 5.5, it is easy to see that most of the parameters are affected very little in comparison to those that are affected the most. A group of 3 parameters, L_{max}, ρ, and η, are affected in the range of 4.2-4.5 percentage points. Next, a pair of 2 parameters, Y_H and L_0, are affected in the range of 0.85-1.0 percentage points. The rest of the parameters are affected less than 0.55 percentage points. An overview of the result of the sensitivity analysis can be obtained by looking at a color plot of the results, see Figure 5.6; it becomes clear that only a few parameter/output-pairs account for the greater part of the uncertainty. To get a more detailed view, still keeping the perspective, we can take a closer look at the 10 parameters with the largest total uncertainty in another color plot, see Figure 5.7.
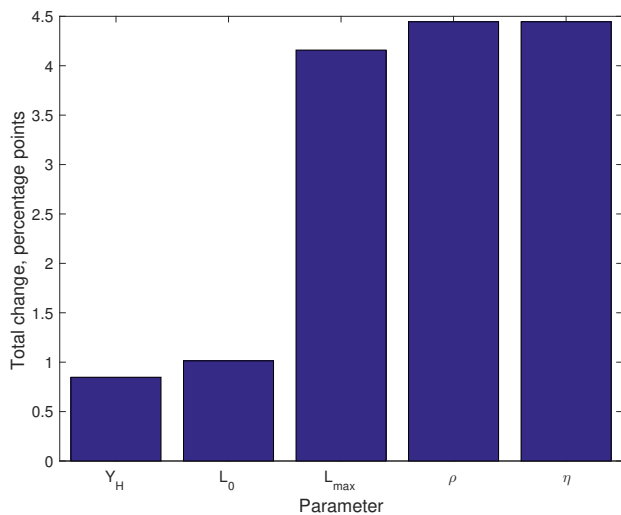
Figure 5.2: The total sensitivity of the five most sensitive parameters, with respect to the sum of the absolute values of the obtained percentage changes in the outputs.
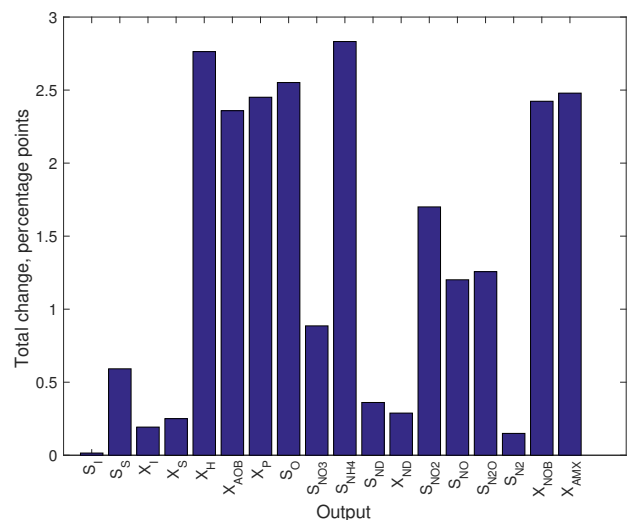
Figure 5.3: The sum of all the sensitivity coefficients of the parameters in each of the outputs.
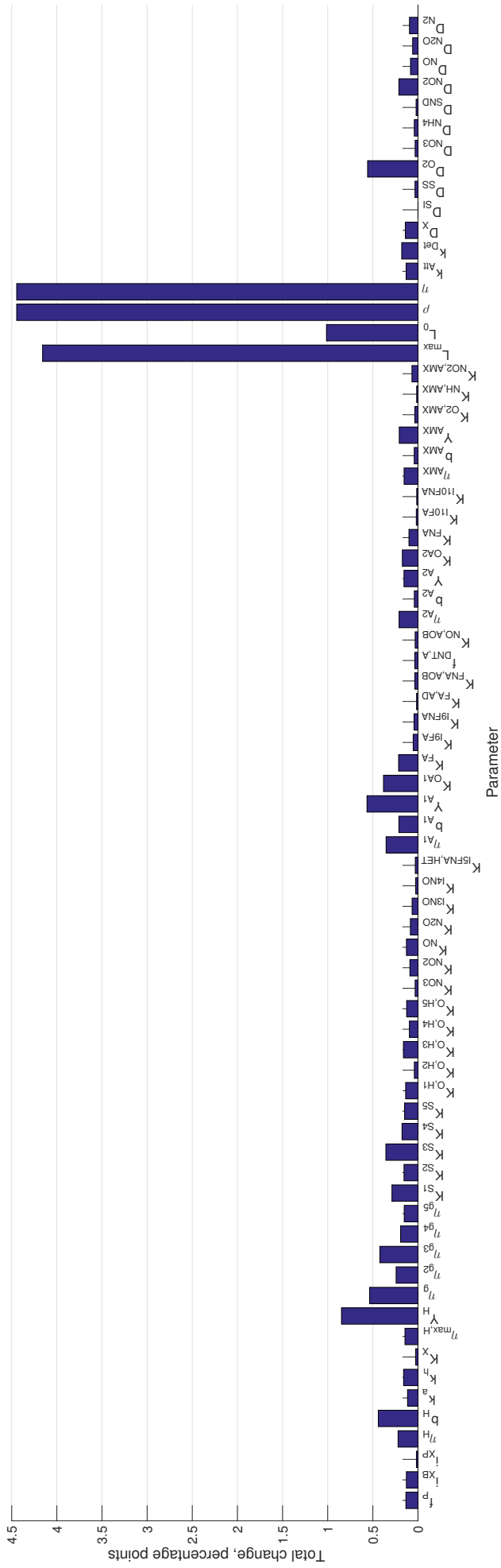
Figure 5.4: The total sensitivity of all the parameters, summed over the outputs, order as in Table 3.3.
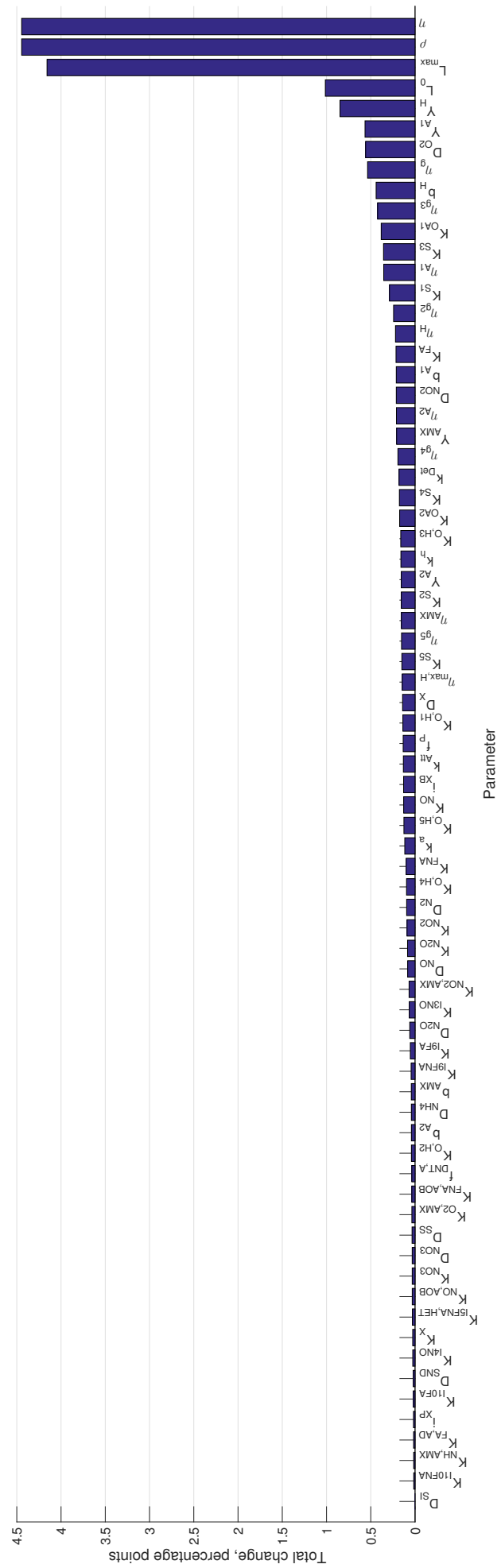
Figure 5.5: The total sensitivity of all the parameters, summed over the outputs, sorted in order of ascending total sensitivity, summed over all the outputs.

27
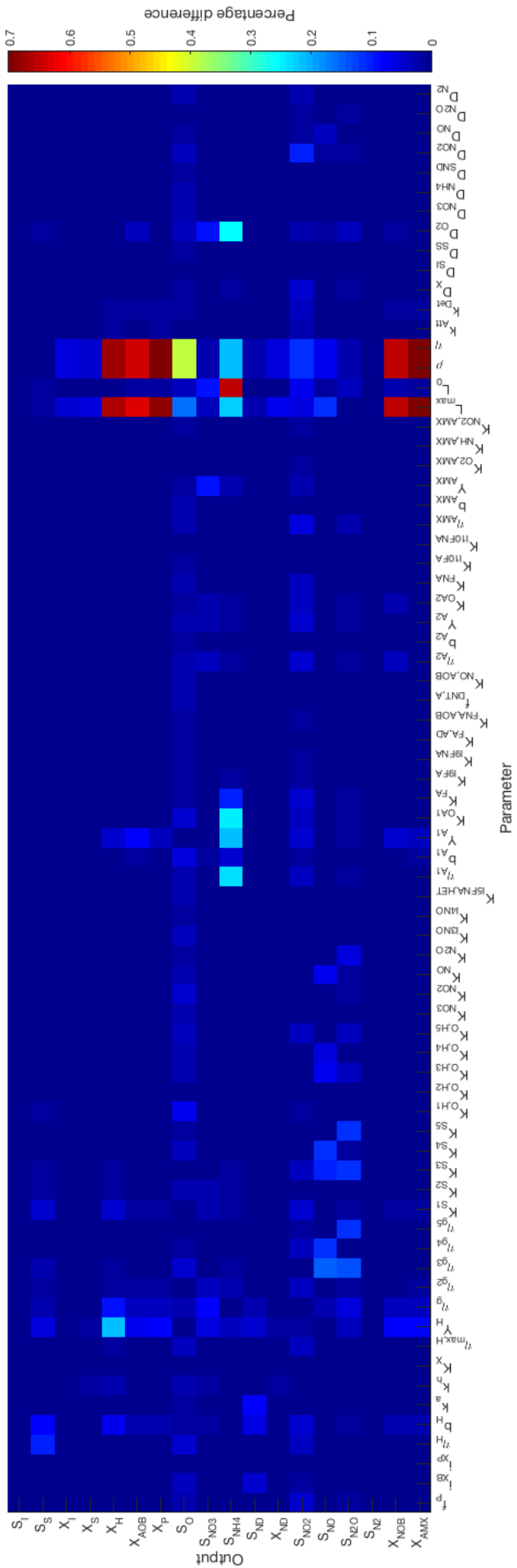
Figure 5.6: A color plot of the sensitivity coefficients for all the parameter/output-pairs.
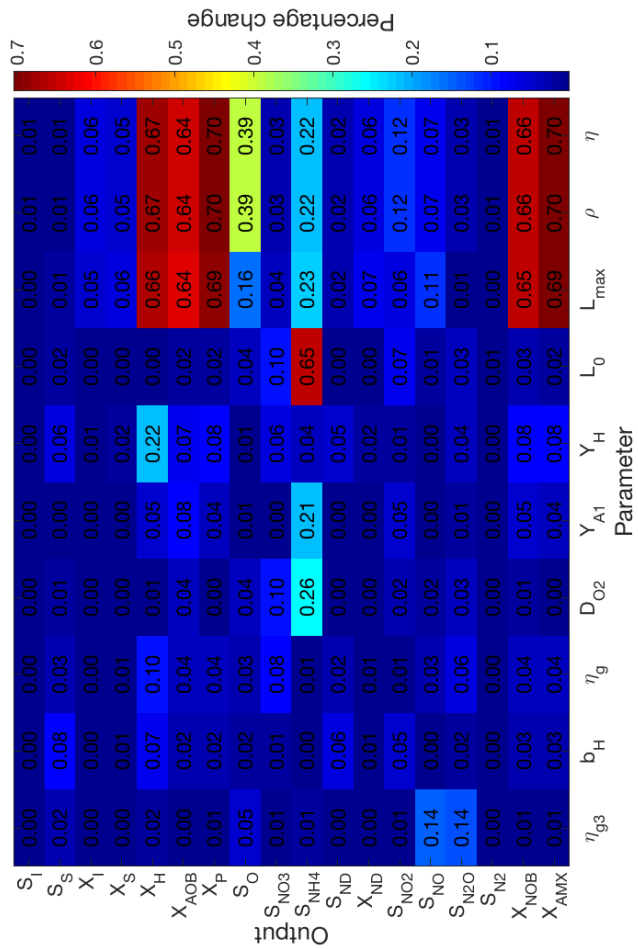
Figure 5.7: A color plot with the sensitivity coefficients of 10 of the most sensitive parameters for all the outputs.

5.3 Calibration

The maximum total FIT was found to be -4.53. The corresponding parameter values are shown in Table 5.1 along with the nominal parameter values as a comparison. The plots of MBBR anammox from a model run with the calibrated parameter values can be seen in Figure 5.8. In plot C, F, and H in Figure 5.8, the measurements, the simulated values before calibration, and the simulated values after calibration, can be seen for the evaluated outputs. In plot C, showing the N_2O in the effluent, we can see that there has been almost no change in the simulated output when comparing the non-calibrated simulation to the calibrated simulation. In plot F, showing the NH_4^+ in the effluent, a major improvement can be seen in the output from the calibrated simulation compared to the non-calibrated simulation; the simulated output fits almost perfectly with the measurements in the calibrated simulation. Looking at plot H, showing the N_2O in the off-gas emission, a small improvement can be seen in the output from the calibrated simulation in comparison to the output from the non-calibrated simulation; the parts of the curve from the calibrated simulation that are slightly flat are closer to the measurements with than the non-calibrated simulation.

Parameter	Nominal value	Calibrated value	Unit
η	0.5	0.2969	-
ρ	5e4	4.656e4	g TS /m^3
L_{max}	1.2	1.785	mm
L_0	56	71.99	μm
Y_H	0.6	0.6632	g cellCOD/(g COD)

Table 5.1: The parameter values of the five most sensitive parameters giving the best FIT according to the calibration, along with their original values.

The distributions of FIT, both the individual and the total, for all the simulations during the calibration are shown in Figure 5.9. In Figure 5.9a, showing the distribution of the FIT of NH_4^+ in the effluent, most simulations gave a FIT-value around -30; still, a significant number of FITs are close to 1. In Figure 5.9b, showing the distribution of the FIT of N_2O in the off-gas emission, only a few simulations gave a FIT less than -1, and many simulations gave a FIT close to 1. In Figure 5.9c, showing the distribution of the FIT of N_2O in the effluent, none of the simulations gave a FIT higher than -3.6 and that most of the FITs are around -4.4. In the Figure 5.9d, the total FIT for the simulations are shown. Evidently, there is a significant amount of simulations that gave a total FIT close to the optimal one.
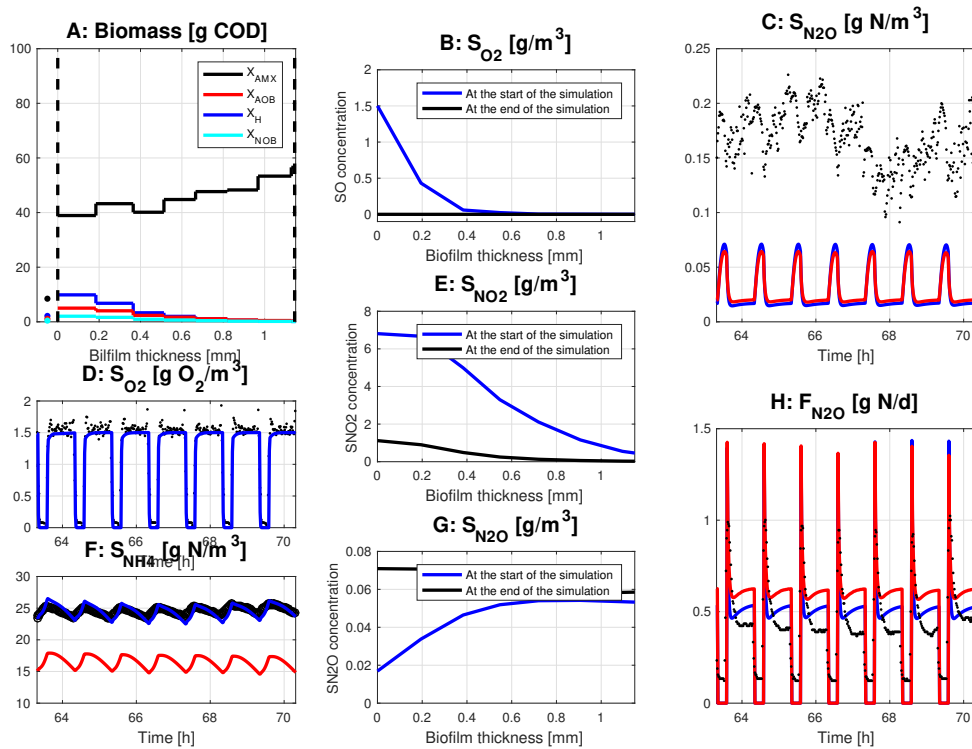
Figure 5.8: The outputs of the model with calibrated parameter values, plotted as in Figure 5.1, which compares the outputs of the calibrated model with the outputs of the model with the nominal values. The red lines in figure C, F, and H is from the simulation with the non-calibrated parameter values, same as in 5.1.
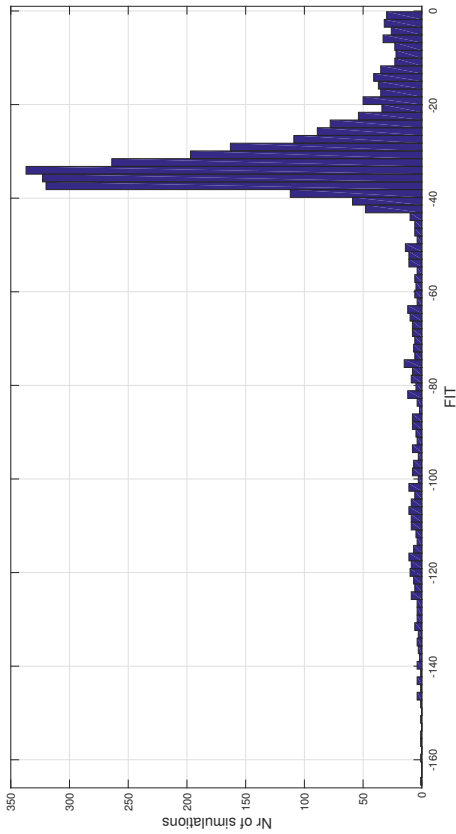
(a) Histogram of the distribution of the FIT from the calibration of NH_4^+ in the effluent.
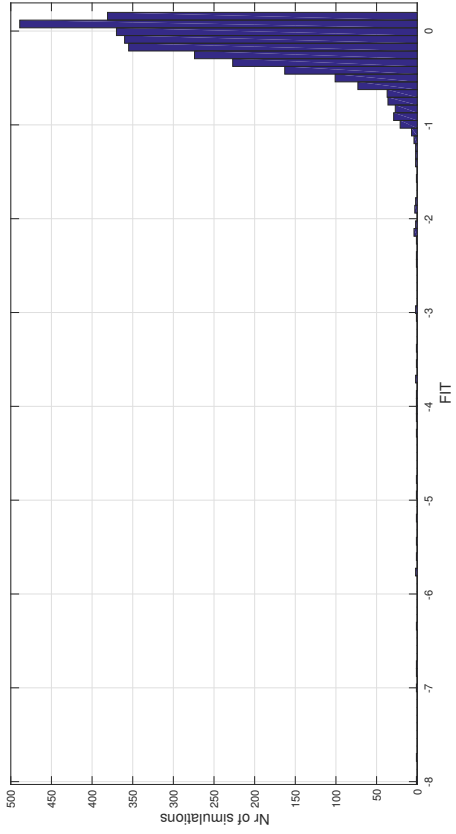
(b) Histogram of the distribution of the FIT from the calibration of N_2O in the off-gas emission.
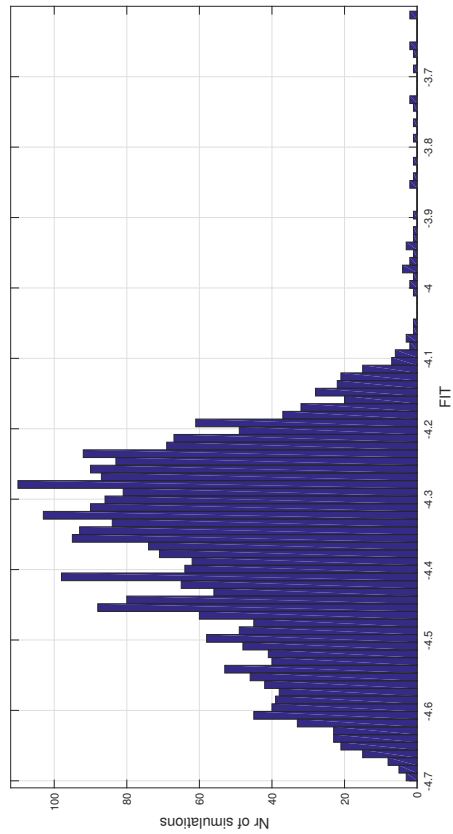
(c) Histogram of the distribution of the FIT from the calibration of N_2O in the effluent.
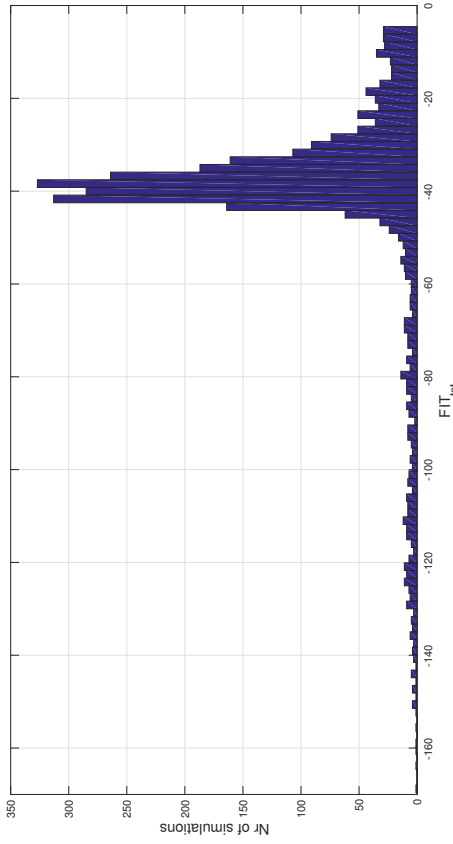
(d) Histogram of the distribution of the total FIT, which is the sum of the individual FITs.

Figure 5.9: Histograms of distribution of the individual FITs and the total FIT.

Chapter 6

Discussion

6.1 Reproduction of results

It took a substantial amount of time to implement the model and make it work properly – even though most of the code was provided. Lindblom should have been contacted at an earlier stage of the project in order to avoid this time-consuming issue.

When comparing figure 3 in (Lindblom et al. 2016) to my result in Figure 5.1 there are some clear yet minor differences, as mentioned in section 5.1. A known source of these variations is the reference input used to the PID controller in the model; Lindblom used the monitored DO concentration from the measurements as input to the controller used in the model, whereas I used a constant value within the periods. In plot F in Figure 5.1 it might look as the deviation of 7 g N/m^3 is large, but in view that the influent of NH$_4{}^+$ is 769 g N/m^3 the deviation of the reduced amount of NH$_4{}^+$ is only 2.2%.

6.2 Sensitivity analysis

As stated in section 5.2, η, ρ, L_{max}, L_0, and Y_H are the five most sensitive parameters of the model. At this point, it is fair to ask why these specific parameters are the most sensitive. Looking at what these parameters control, the answer could be found in that the first four describe fundamental dynamics of the biofilm. η describes the porosity of the biofilm, thereby controlling the rate of the mass transports within the biofilm, thus significantly influencing many processes. The impact that the biofilm density, ρ, has on the processes within the biofilm is a complex matter. A fair assumption of its effect is to suppose that increased biofilm density would increase nutrient consumption caused by the increased amount of microorganisms. However, that is not the case since the increased biomass density decreases the over-all diffusivity in the biofilm, thereby halting the effect of the increased microorganism population (Lewandowski and Beyenal 2007). L_{max} describes the maximum biofilm thickness at which biomass starts to fall off. This parameter is crucial since it affects an important aspect of the dynamics of the biofilm. L_0 is the thickness of the boundary layer of the biofilm. A such, it regulates the diffusion of soluble compounds into and out from the biofilm; therefore, it is not surprising that it is sensitive to uncertainties. Y_H is the only one of the five most sensitive parameters that does not describe an aspect of the biofilm dynamics. Instead, it describes the heterotrophic yield which is involved in all the reactions with the soluble components, which might in part explain why it is sensitive to uncertainties.

$K_L a$ is the only parameter that is not part of the sensitivity analysis. The reason being that it is the output of the controller. If the value of $K_L a$ would have been fixed it should have been included in the

calibration to.

What has not been investigated in the sensitivity analysis is how the perturbations of the parameter values interact with each other. This was because OAT does not explore the effect of simultaneous changes of parameter values. A variance-based sensitivity analysis could have been made in order to do so; then it might have been discovered that simultaneous perturbations of a pair or a group of parameter values together create large variations in the output.

6.3   Calibration

The calibration did not find any parameter set that made a good fit possible to achieve between the measurements and the simulation of the N_2O in the effluent. The outputs of the simulations did not appear to be significantly affected by the changes of parameter values either; the FIT did not show any larger variations. The reasons for that is unknown, but some hypotheses are that: the measurements are erroneous; the parameters varied during the calibration are not the ones governing the dynamics of the N_2O in the effluent; some dynamic, affecting the dynamics of the N_2O in the effluent, is missing in the model.

Only three outputs with experimental values were available for this calibration. For a more accurate result more experimental data should be fetched and included. More experimental data would also have made a proper validation of the model possible. Furthermore, a calibration with more simulations would give a better and more precise result regarding what the parameter values should be – resulting in a better FIT.

6.4   The anammox model

Since only a limited amount of experimental data were available, no solid conclusion can be reached about whether Lindblom's model is a good basis for further development of a model for MBBR anammox. Lindblom's aim with this model was primarily to create a good model that included N_2O, which is known to be difficult to model. Therefore, even though a good fit between the measurements and the simulations of the N_2O in the effluent could not be achieved from the calibration, the rest of the model states seem to model the system in a correct way. The simulation of the NH_4^+ in the effluent corresponded almost exactly to the simulation after it had been calibrated. Also, the simulations of the amount of biomass in the biofilm layers with different distances from the bulk is consistent with the theory concerning the biofilm dynamics. My conclusion is therefore that the model has good potential to mimic the anammox process with MBBR through further development and validation.

6.5   Improvements

According to (Henze 2008), the process rates should only include the minimum factor, i.e. the limiting factor, in order to achieve the most accurate result. This is not the case in Lindblom's model and might therefore be implemented to accomplish a better performance.

In Lindblom's model, the pH value and the temperature in the reactor are assumed to be constant. In reality, both the pH value and temperature varies and also has high influence in the process dynamics (Xing et al. 2016), (Henze et al. 1987). To implement the pH dependencies and the temperature dependencies, many of changes have to be made, and the complexity of the model will grow substantially.

Still, it might be worth the effort when considering further development of the model to increase the correctness of the model.

Additional possible proposals for improvements are: support for other types of regulators than PID, for example Fuzzy Logic Control (FLC), Model Predictive Control (MPC); support for other types of aeration feedback - like ammonium-based control; other aeration patterns than just the on/off-pattern should be possible to simulate.

Chapter 7

Conclusions

In this thesis, the one-step anammox process with MBBR, proposed by Erik Lindblom in (Lindblom et al. 2016) has been evaluated. A calibration has successfully been done of the five most sensitive parameters, although one of the model outputs could not been satisfactorily calibrated to the experimental data. The model can be stated to have good potential as a basis for future developments of a model for the process.

Besides the validation and calibration against more experimental data, possible future work for this model includes adjusted process rates and the inclusion of pH dependence and temperature dependence.

Bibliography

[1] A.H. Devol. "Nitrogen cycle: solution to a marine mystery". In: *Nature* 422.6932 (2003), pp. 575–576.

[2] J. Foley et al. *N2O and CH4 Emission from Wastewater Collection and Treatment Systems: State of the Science Report and Technical Report.* Tech. rep. London, UK.: Global Water Research Coalition, 2015.

[3] W. Gujer, M. Henze, T. Mino, and M.C M. van Loosdrecht. "Activated Sludge Model No. 3". In: *Wat. Sci. Technol.* 39.1 (1999), pp. 183–193.

[4] X. Hao, J.J. Heijnen, and M.C M. van Loosdrecht. "Sensitivity analysis of a biofilm model describing a one-stage completely autotrophic nitrogen removal (CANON) process". In: *Biotechnology and Bioengineering* 77.3 (2002), pp. 266–277.

[5] M. Henze. *Biological Wastewater Treatment: Principles, Modelling and Design.* IWA Pub, 2008.

[6] M. Henze, C.P.L. Grady, W. Gujer, G.v.R. Marais, and T. Matsuo. *Activated Sludge Model No. 1.* Tech. rep. Scientific and Technical Report No. 1. London,UK.: IAWQ, 1987.

[7] M. Henze, W. Gujer, T. Mino, T. Matsuo, M.C.M. Wentzel, and G.v.R. Marais. *Activated Sludge Model No. 2.* Tech. rep. Scientific and Technical Report No. 3. London,UK.: IAWQ, 1995.

[8] M. Henze, W. Gujer, T. Mino, T. Matsuo, M.C.M. Wentzel, G.v.R. Marais, and M.C M. van Loosdrecht. "Activated Sludge Model No.2d. ASM2D". In: *Water Science and Technology* 39.1 (1999), pp. 165–182.

[9] W.C. Hiatt and C.P. Leslie Grady. "An Updated Process Model for Carbon Oxidation, Nitrification, and Denitrification". In: *Water Environment Research* 80.11 (2008), pp. 2145–2156.

[10] B. Kartal et al. "Molecular mechanism of anaerobic ammonium oxidation". In: *Nature* 479.7371 (2011), pp. 127–130.

[11] J.G. Kuenen. "Anammox bacteria: From discovery to application". In: *Nature Reviews Microbiology* 6.4 (2008), pp. 320–326.

[12] Z. Lewandowski and H. Beyenal. *Fundamentals of Biofilm Research.* CRC Press, 2007.

[13] E. Lindblom, M. Arnell, X. Flores-Alsina, F. Stenstrom, D.J.I. Gustavsson, J. Yang, and U. Jeppsson. "Dynamic modelling of nitrous oxide emissions from three Swedish sludge liquor treatment systems". In: *Water Science and Technology* 73.4 (2016), p. 798.

[14] E. Lindblom, M. Arnell, and U. Jeppsson. *Modellering av lustgasemissioner från SBR- och anammoxprocesser för rejektvattenbehandling.* Swedish. Tech. rep. 17. Svenskt Vatten Utveckling, 2015.

[15] K.E. Mampaey, B. Beuckels, M.J. Kampschreur, R. Kleerebezem, M.C.M. van Loosdrecht, and E.I.P. Volcke. "Modelling nitrous and nitric oxide emissions by autotrophic ammonia-oxidizing bacteria". In: *Environ. Technol.* 34.12 (2013), pp. 1555–1566.

[16]   Naturvårdsverket. "Rening av avloppsvatten i Sverige 2014". Swedish. In: (2014).

[17]   E. Plaza, F. Persson, B.M. Wilén, and R. Sultana. *Användning av Anammox för en förbättrad kväveavskiljning vid avloppsverk*. Swedish. Tech. rep. 18. Svenskt Vatten Utveckling, 2015.

[18]   W.R.L. Van der Star. "Growth and Metabolism of Anammox Bacteria". PhD thesis. TU Delft, 2008.

[19]   M. Strous, J.J. Heijnen, J.G. Kuenen, and M.S.M. Jetten. "The sequencing batch reactor as a powerful tool for the study of slowly growing anaerobic ammonium-oxidizing microorganisms". In: *Applied Microbiology and Biotechnology* 50.5 (1998), pp. 589–596.

[20]   J. Trela, E. Płaza, B. Hultman, G. Cema, J. Bosander, and E. Levlin. *Utvärdering av enstegsprocess för deammonifikation*. Swedish. Tech. rep. 18. Svenskt Vatten Utveckling, 2008.

[21]   B. Xing, Q. Guo, x. Jiang, Q. Chen, P. Li, W. Ni, and R. Jin. "Influence of preservation temperature on the characteristics of anaerobic ammonium oxidation (anammox) granular sludge". In: *Applied Microbiology and Biotechnology* 100.10 (2016), pp. 4637–4649.

Appendix A

MATLAB-code

A.1   Sensitivity analysis

sensitivity_analysis.m

```matlab
% Sensitivity analysis, 10% pertubation

%% Init
init_sim;
simOut = sim('mbbr_amx_O2reg');
mbbr = simOut.get('mbbr');
a_init = mbbr(end,1:nbrOfStates); % Save last states
SOAMXreg_kvot = simOut.get('SOAMXreg_kvot'); % States for the controller
reg_init(1)=SOAMXreg_kvot(end,4); % Save last state
reg_init(2)=SOAMXreg_kvot(end,5); % Save last state


% Simulate 2 more days without changes, save last hour's results
ANAMMOXINIT_ASMN(1:nbrOfStates) = a_init; % State after 53 days as init state
SOAMXintstate = reg_init(1);
SOAMXawstate = reg_init(2);
tend = 2;
simOut = sim('mbbr_amx_O2reg');
one_h_samp_nr = round(1/(t_tick*24))-1; % Nr of samples in one hour
eff = simOut.get('eff');
eff0 = eff(end-one_h_samp_nr:end,:); % Baseline values
outputs = [1:12 17:21 25];
l = length(outputs);

% Order for process parameter vector PAR_ASMN (ASMPAR in S-function)
asm_order = [17:19 1 5 11:15 10 26:45 75 47 49 51 55 53 57 58 87 71 73 ...
             74 48 50 52 56 54 59 60 76 77 81 78:80];
% Order for BIOFILM
bio_order = [3 7 8 6 9 10 22];
% Order for DIFFUSIONPAR
dif_order = [1 2 8:11 17:20];

l_par = cumsum([length(asm_order) length(bio_order) length(dif_order)]);
sens_res = zeros(l,l_par(end));
inc = 1.1; % perturbation, value to multiply the parameters with

par_asmn0 = PAR_ASMN;
biofilmpar0 = BIOFILMPAR;
diffusionpar0 = DIFFUSIONPAR;
```

```
40
41  %% Change and simulate, order as in the thesis parameter list
42
43  for i = 1:length(asm_order)
44      ANAMMOXINIT_ASMN(1:nbrOfStates) = a_init;
45      SOAMXintstate=reg_init(1);
46      SOAMXawstate=reg_init(2);
47      clear eff
48      PAR_ASMN(asm_order(i)) = par_asmn0(asm_order(i))*inc;  %#ok<*SAGROW>
49      simOut = sim('mbbr_amx_O2reg');
50      eff = simOut.get('eff');
51      eff = eff(end-one_h_samp_nr:end,:);
52      for j = 1:l
53          sens_res(j,i) = mean(abs(eff(:,outputs(j)) - eff0(:,outputs(j)))...
54              ./ eff0(:,outputs(j)));
55      end
56      PAR_ASMN(asm_order(i)) = par_asmn0(asm_order(i));
57  end
58
59
60  for i = 1:length(bio_order)
61      ANAMMOXINIT_ASMN(1:nbrOfStates) = a_init;
62      SOAMXintstate=reg_init(1);
63      SOAMXawstate=reg_init(2);
64      clear eff
65      BIOFILMPAR(bio_order(i)) = biofilmpar0(bio_order(i))*inc;
66      simOut = sim('mbbr_amx_O2reg');
67      eff = simOut.get('eff');
68      eff = eff(end-one_h_samp_nr:end,:);
69      for j = 1:l
70          sens_res(j,i+l_par(1)) = mean(abs(eff(:,outputs(j)) - ...
71              eff0(:,outputs(j)))./eff0(:,outputs(j)));
72      end
73      BIOFILMPAR(bio_order(i)) = biofilmpar0(bio_order(i));
74  end
75
76  for i = 1:length(dif_order)
77      ANAMMOXINIT_ASMN(1:nbrOfStates) = a_init;
78      SOAMXintstate=reg_init(1);
79      SOAMXawstate=reg_init(2);
80      clear eff
81      DIFFUSIONPAR(dif_order(i)) = diffusionpar0(dif_order(i))*inc;
82      simOut = sim('mbbr_amx_O2reg');
83      eff = simOut.get('eff');
84      eff = eff(end-one_h_samp_nr:end,:);
85      for j = 1:l
86          sens_res(j,i+l_par(2)) = mean(abs(eff(:,outputs(j)) - ...
87              eff0(:,outputs(j)))./eff0(:,outputs(j)));
88      end
89      DIFFUSIONPAR(dif_order(i)) = diffusionpar0(dif_order(i));
90  end
```

plot_sens.m

```
1  % Generates 6 plots, visualizing the results from the sensitivity analysis
2
3  % Labels
4  outputs = {'S_I' 'S_S' 'X_I' 'X_S' 'X_H' 'X_{AOB}' 'X_P' 'S_O' ...
5      'S_{NO3}' 'S_{NH4}' 'S_{ND}' 'X_{ND}' 'S_{NO2}' 'S_{NO}' ...
6      'S_{N2O}' 'S_{N2}' 'X_{NOB}' 'X_{AMX}'};
```

```matlab
7  params = {'f_P' 'i_{XB}' 'i_{XP}' '\eta_H' 'b_H' 'k_a' 'k_h' 'K_X'...
8      '\eta_{max,H}' 'Y_H' '\eta_{g}' '\eta_{g2}' '\eta_{g3}'...
9      '\eta_{g4}' '\eta_{g5}' 'K_{S1}' 'K_{S2}' 'K_{S3}' 'K_{S4}'...
10     'K_{S5}' 'K_{O,H1}' 'K_{O,H2}' 'K_{O,H3}' 'K_{O,H4}'...
11     'K_{O,H5}' 'K_{NO3}' 'K_{NO2}' 'K_{NO}' 'K_{N2O}' 'K_{I3NO}'...
12     'K_{I4NO}' 'K_{I5FNA,HET}' '\eta_{A1}' 'b_{A1}' 'Y_{A1}'...
13     'K_{OA1}' 'K_{FA}' 'K_{I9FA}' 'K_{I9FNA}' 'K_{FA,AD}'...
14     'K_{FNA,AOB}' 'f_{DNT,A}' 'K_{NO,AOB}' '\eta_{A2}' 'b_{A2}'...
15     'Y_{A2}' 'K_{OA2}' 'K_{FNA}' 'K_{I10FA}','K_{I10FNA}'...
16     '\eta_{AMX}' 'b_{AMX}' 'Y_{AMX}' 'K_{O2,AMX}' 'K_{NH,AMX}'...
17     'K_{NO2,AMX}' 'L_{max}' 'L_0' '\rho' '\eta' 'k_{Att}'...
18     'k_{Det}' 'D_X' 'D_{SI}' 'D_{SS}' 'D_{O2}' 'D_{NO3}' 'D_{NH4}'...
19     'D_{SND}' 'D_{NO2}' 'D_{NO}' 'D_{N2O}' 'D_{N2}'};
20
21 % Calculations
22 s_p = sum(sens_res,1); %Total change in the parameters, percentage points
23 [s_p_asc,I] = sort(s_p); %Sort parameter values ascending
24 params_asc = params(I); %Sort parameter names
25 s_o = sum(sens_res,2); %Total change in the outputs, percentage points
26 sens_res_asc = sens_res(:,I); %Sort res by params in asc. order of tot sens.
27 sens_asc_red = sens_res_asc(:,end-9:end); %The 10 most sensitive (tot) parameters
28
29
30 % Color plot, all parameters and outputs
31 figure(1)
32 imagesc(sens_res) % Create color plot
33 colormap(jet); % Set colors
34 c = colorbar;
35 set(gca,'XTick',1:length(params),'XTickLabel', params',...
36     'XTickLabelRotation',90,'YTick',1:length(outputs),...
37     'YTickLabel',outputs','FontSize',12)
38 ylabel(c,'Percentage difference','FontSize',14)
39 xlabel('Parameter','FontSize',14)
40 ylabel('Output','FontSize',14)
41
42 % Total sensitivity of parameters, order as in paper
43 figure(2)
44 bar(1:length(s_p),s_p)
45 set(gca,'XTick',1:length(params),'XTickLabel',params', ...
46     'XTickLabelRotation',90,'FontSize',12)
47 xlabel('Parameter','FontSize',14)
48 ylabel('Total change, percentage points','FontSize',14)
49
50 % Total sensitivity of parameters, asc order of sensitivity
51 figure(3)
52 bar(1:length(s_p_asc),s_p_asc)
53 set(gca,'XTick',1:length(params_asc),'XTickLabel',params_asc', ...
54     'XTickLabelRotation',90,'FontSize',12)
55 xlabel('Parameter','FontSize',14)
56 ylabel('Total change, percentage points','FontSize',14)
57
58 % Total sensitivity of the 5 most sensitive parameters
59 figure(4)
60 bar(1:5,s_p_asc(end-4:end))
61 set(gca,'XTick',1:length(params_asc(end-4:end)),'XTickLabel',...
62     params_asc(end-4:end),'FontSize',12)
63 xlabel('Parameter','FontSize',14)
64 ylabel('Total change, percentage points','FontSize',14)
65
66 % Sum of all change in parameters per output
67 figure(5)
```

```
68  bar(1:length(s_o),s_o)
69  set(gca,'XTick',1:length(outputs),'XTickLabel',outputs', ...
70      'XTickLabelRotation',90,'FontSize',12)
71  xlabel('Output','FontSize',14)
72  ylabel('Total change, percentage points','FontSize',14)
73
74  % Color plot of the 10 most sensitive (tot) parameters
75  figure(6)
76  imagesc(sens_asc_red);
77  colormap(jet); % Set colors
78  textStrings = cellfun(@(x)({num2str(x,'%0.2f')}), num2cell(sens_asc_red'));
79  [x_l,y_l] = size(sens_asc_red);
80  [y,x] = meshgrid(1:x_l,1:y_l);    % Create x and y coordinates for the strings
81  text(x(:),y(:),textStrings(:),'HorizontalAlignment','center','FontSize', 22);
82  set(gca,'XTick',1:length(params_asc(end-9:end)),...
83      'XTickLabel',params_asc(end-9:end)','YTick',1:length(outputs),...
84      'YTickLabel',outputs','FontSize', 22)
85  c = colorbar;
86  ylabel(c,'Percentage change','FontSize', 26)
87  xlabel('Parameter','FontSize',26)
88  ylabel('Output','FontSize',26)
```

A.2   Calibration

calibration.m

```
1   init_sim;
2   mdl = 'mbbr_amx_O2reg';
3   if (¬bdIsLoaded(mdl))
4       load_system(mdl);
5   end
6   assignin('base','BIOFILMPAR',BIOFILMPAR);
7   assignin('base','PAR_ASMN',PAR_ASMN);
8   assignin('base','ANAMMOXINIT_ASMN',ANAMMOXINIT_ASMN);
9   assignin('base','CONSTINFLUENT_MBBR_AMX',CONSTINFLUENT_MBBR_AMX);
10  assignin('base','TEMPMODEL',TEMPMODEL);
11  assignin('base','TSS_VECTOR',TSS_VECTOR);
12  assignin('base','DIFFUSIONPAR',DIFFUSIONPAR);
13  assignin('base','PART_VECTOR',PART_VECTOR);
14  assignin('base','EQ_LAYERS',EQ_LAYERS);
15  assignin('base','KLa_mbbr',KLa_mbbr);
16  assignin('base','pH_mbbr',pH_mbbr);
17  assignin('base','KSOAMX',KSOAMX);
18  assignin('base','SOAMXintstate',SOAMXintstate);
19  assignin('base','KLaAMXoffset',KLaAMXoffset);
20  assignin('base','KLaAMX_max',KLaAMX_max);
21  assignin('base','TiSOAMX',TiSOAMX);
22  assignin('base','TtSOAMX',TtSOAMX);
23  assignin('base','SOAMXawstate',SOAMXawstate);
24  assignin('base','useantiwindupSOAMX',useantiwindupSOAMX);
25  assignin('base','nbrOfOutputs',nbrOfOutputs);
26  assignin('base','nbrOfLayers',nbrOfLayers);
27  assignin('base','nbrOfStates',nbrOfStates);
28  assignin('base','tstart',tstart);
29  assignin('base','tend',tend);
30  assignin('base','t_tick',t_tick);
31
32  rtp = Simulink.BlockDiagram.buildRapidAcceleratorTarget(mdl);
33
```

```matlab
34   t1=52.763; % days
35   nr_of_sim = 3000;
36   variance = 0.5; % 50% variance of the parameters
37
38   % Experimental values to compare against
39   load 140705_dyn g_n2o n2o_vatten nh t_meas
40   ind = find(t_meas*24>=(t1—3/24—50)*24 & t_meas*24<=(t1+4/24—50)*24);
41   nh = nh(ind);
42   g_n2o = g_n2o(ind);
43   s_n2o = n2o_vatten(ind);
44
45   l_p = 5;
46   lhs = lhsdesign(nr_of_sim,5);
47   lhs1 = lhs(:,1); % Sliced variables not allowed with parfor —> split lhs
48   lhs2 = lhs(:,2);
49   lhs3 = lhs(:,3);
50   lhs4 = lhs(:,4);
51   lhs5 = lhs(:,5);
52   fit_par1 = zeros(1,nr_of_sim); % Sliced variables not allowed with parfor
53   fit_par2 = zeros(1,nr_of_sim);
54   fit_par3 = zeros(1,nr_of_sim);
55   fit_tot = zeros(1,nr_of_sim);
56
57   % Generate modified parameter sets
58   bio_var = repmat(BIOFILMPAR,nr_of_sim,1);
59   bio_var(:,3) = BIOFILMPAR(3)*(1 + variance*(lhs1*2 — 1)); % L_max
60   bio_var(:,6) = BIOFILMPAR(6)*(1 + variance*(lhs2*2 — 1)); % eta
61   bio_var(:,7) = BIOFILMPAR(7)*(1 + variance*(lhs3*2 — 1)); % L_0
62   bio_var(:,8) = BIOFILMPAR(8)*(1 + variance*(lhs4*2 — 1)); % rho
63   asm_var = repmat(PAR_ASMN,nr_of_sim,1);
64   asm_var(:,15) = PAR_ASMN(15)*(1 + variance*(lhs5*2 — 1)); % Y_H
65
66   paramSet = cell(1, nr_of_sim);
67   for i = 1:nr_of_sim
68       paramSet{i} = Simulink.BlockDiagram.modifyTunableParameters(rtp, ...
69           'BIOFILMPAR',bio_var(i,:),'PAR_ASMN',asm_var(i,:));
70   end
71
72   parfor i = 1:nr_of_sim
73       assignin('base','BIOFILMPAR',BIOFILMPAR);
74       assignin('base','PAR_ASMN',PAR_ASMN);
75       assignin('base','ANAMMOXINIT_ASMN',ANAMMOXINIT_ASMN);
76       assignin('base','CONSTINFLUENT_MBBR_AMX',CONSTINFLUENT_MBBR_AMX);
77       assignin('base','TEMPMODEL',TEMPMODEL);
78       assignin('base','TSS_VECTOR',TSS_VECTOR);
79       assignin('base','DIFFUSIONPAR',DIFFUSIONPAR);
80       assignin('base','PART_VECTOR',PART_VECTOR);
81       assignin('base','EQ_LAYERS',EQ_LAYERS);
82       assignin('base','KLa_mbbr',KLa_mbbr);
83       assignin('base','pH_mbbr',pH_mbbr);
84       assignin('base','KSOAMX',KSOAMX);
85       assignin('base','SOAMXintstate',SOAMXintstate);
86       assignin('base','KLaAMXoffset',KLaAMXoffset);
87       assignin('base','KLaAMX_max',KLaAMX_max);
88       assignin('base','TiSOAMX',TiSOAMX);
89       assignin('base','TtSOAMX',TtSOAMX);
90       assignin('base','SOAMXawstate',SOAMXawstate);
91       assignin('base','useantiwindupSOAMX',useantiwindupSOAMX);
92       assignin('base','nbrOfOutputs',nbrOfOutputs);
93       assignin('base','nbrOfLayers',nbrOfLayers);
94       assignin('base','nbrOfStates',nbrOfStates);
```

```
95      assignin('base','tstart',tstart);
96      assignin('base','tend',tend);
97      assignin('base','t_tick',t_tick);
98
99      simOut = sim(mdl,'StartTime','0','StopTime','53',...
100         'RapidAcceleratorUpToDateCheck','off',...
101         'RapidAcceleratorParameterSets',paramSet{i});
102     eff = simOut.get('eff');
103     offgas_mbbr = simOut.get('offgas_mbbr');
104     t_sim = simOut.get('t');
105
106     ind_sim = find((t_sim+2)*24≥(t1—3/24—50)*24 & (t_sim+2)*24≤(t1+4/24—50)*24);
107     nh_sim = eff(ind_sim,10);
108     g_n2o_sim = offgas_mbbr(ind_sim,2);
109     s_n2o_sim = eff(ind_sim,19);
110
111     fit_par1(1,i) = goodnessOfFit(nh_sim,nh,'NRMSE');
112     fit_par2(1,i) = goodnessOfFit(g_n2o_sim,g_n2o,'NRMSE');
113     fit_par3(1,i) = goodnessOfFit(s_n2o_sim,s_n2o,'NRMSE');
114     fit_tot(1,i) = sum(fit_par1(1,i)+fit_par2(1,i)+fit_par3(1,i));
115 end
```

A.3   Help functions/scripts

find_cal_par.m

```
1  % Script for fetching the parameter values from the calibration that gave
2  % the highest total FIT.
3
4  r = load('cal_res.mat'); % Saved output from the calibration
5  r = r.j; % Results saved as 'j' in cal_res.mat
6  [max_fit,ind] = max(r.fit_tot);
7  best_lhs = r.lhs(ind,:);
8  new_par_val = zeros(1,5);
9
10 new_par_val(1) = r.BIOFILMPAR(3)*(1 + r.variance*(best_lhs(1)*2 — 1)); %L_max
11 new_par_val(2) = r.BIOFILMPAR(6)*(1 + r.variance*(best_lhs(2)*2 — 1)); %eta
12 new_par_val(3) = r.BIOFILMPAR(7)*(1 + r.variance*(best_lhs(3)*2 — 1)); %L_0
13 new_par_val(4) = r.BIOFILMPAR(8)*(1 + r.variance*(best_lhs(4)*2 — 1)); %rho
14 new_par_val(5) = r.PAR_ASMN(15)*(1 + r.variance*(best_lhs(5)*2 — 1)); %Y_H
```

Appendix B

Full sensitivity analysis results

	S_I	S_S	X_I	X_S	X_H	X_{AOB}	X_P	S_O	S_{NO3}	S_{NH4}	S_{ND}	X_{ND}	S_{NO2}	S_{NO}	S_{N2O}	S_{N2}	X_{NOB}	X_{AMX}
f_P	1.23e-05	2.64e-03	1.33e-04	1.76e-04	2.44e-03	2.20e-03	5.08e-03	6.58e-03	3.71e-03	1.96e-03	3.98e-04	3.71e-05	1.34e-03	1.84e-03	3.34e-03	2.75e-04	2.08e-03	1.11e-03
i_{XB}	8.41e-07	9.69e-04	1.00e-04	4.51e-06	3.89e-04	1.60e-04	1.49e-03	1.39e-02	5.21e-04	1.13e-02	4.69e-02	2.43e-03	3.98e-02	3.36e-03	1.01e-02	5.11e-03	8.62e-04	1.79e-03
i_{XP}	1.21e-06	2.22e-04	1.25e-05	3.11e-05	3.05e-04	2.12e-04	2.44e-04	1.41e-02	1.52e-04	2.43e-03	2.57e-03	1.03e-04	1.24e-02	6.06e-04	3.57e-03	1.51e-03	1.32e-05	3.48e-04
η_H	1.27e-06	1.01e-01	1.83e-04	6.69e-04	7.96e-03	2.12e-03	2.57e-03	3.18e-02	4.14e-04	8.67e-03	9.28e-04	7.47e-04	3.84e-02	2.12e-03	6.16e-03	5.27e-03	2.24e-03	2.56e-03
b_H	4.20e-05	8.05e-02	2.04e-03	8.74e-03	7.44e-02	2.38e-02	2.55e-02	2.27e-02	1.21e-02	1.01e-02	6.07e-02	8.41e-03	1.91e-03	8.45e-04	2.51e-03	3.44e-04	2.62e-02	2.72e-02
k_a	2.58e-06	6.00e-04	3.21e-05	6.35e-05	5.73e-04	3.90e-04	5.77e-04	1.43e-02	4.61e-04	2.52e-03	8.43e-02	6.29e-05	8.97e-04	4.68e-04	2.58e-04	2.53e-04	2.46e-04	8.33e-04
k_h	4.25e-05	5.65e-03	2.69e-04	1.68e-02	2.83e-02	8.37e-03	2.88e-03	1.04e-02	1.59e-02	5.31e-03	6.54e-04	1.69e-02	3.31e-02	1.32e-03	6.31e-03	3.80e-03	6.81e-03	6.97e-04
K_X	1.47e-05	1.23e-03	1.92e-06	7.84e-04	3.11e-03	2.51e-03	2.80e-04	4.41e-02	3.14e-03	2.57e-03	1.38e-03	7.20e-04	8.53e-03	1.56e-03	3.54e-03	1.44e-03	2.87e-04	4.07e-04
$\eta_{max,H}$	4.66e-05	4.77e-03	1.95e-04	3.48e-03	1.85e-03	6.50e-03	1.93e-03	1.80e-02	1.11e-02	7.85e-03	6.19e-04	3.59e-03	3.88e-02	1.23e-03	9.09e-03	5.11e-03	5.60e-03	2.15e-04
Y_H	1.93e-04	6.03e-02	6.41e-03	1.53e-02	2.14e-01	7.20e-02	8.74e-02	2.04e-02	6.14e-02	4.07e-02	4.77e-02	1.72e-02	1.69e-02	3.24e-03	2.97e-02	1.55e-03	8.06e-02	8.53e-02
η_g	9.18e-05	3.18e-02	2.84e-03	7.04e-03	9.73e-02	3.59e-02	3.83e-02	2.12e-02	8.29e-02	9.97e-03	2.34e-02	7.87e-03	1.33e-02	2.76e-02	5.99e-02	3.00e-03	3.52e-02	3.68e-02
η_{g2}	1.91e-05	2.13e-02	6.79e-04	1.64e-03	2.30e-02	1.12e-02	9.17e-03	1.25e-02	4.17e-02	2.63e-02	3.91e-05	1.86e-03	2.57e-02	8.07e-03	1.21e-02	3.54e-03	8.29e-03	9.02e-03
η_{g3}	8.45e-06	2.25e-02	4.76e-04	1.50e-03	2.01e-02	4.16e-03	6.52e-03	3.50e-02	7.14e-03	1.50e-02	2.67e-04	1.67e-03	1.29e-02	1.45e-01	1.41e-01	1.98e-03	6.31e-03	6.47e-03
η_{g4}	8.71e-07	2.85e-03	4.85e-05	1.67e-04	2.14e-03	4.23e-04	6.77e-04	1.33e-02	6.70e-04	3.21e-03	1.87e-04	1.88e-04	1.26e-02	1.10e-01	2.12e-02	1.57e-03	6.95e-04	7.36e-04
η_{g5}	6.40e-07	6.56e-04	2.97e-05	2.07e-04	2.59e-03	9.31e-04	2.76e-04	6.87e-02	1.55e-03	6.09e-03	4.53e-04	2.26e-04	3.32e-02	5.36e-03	1.18e-01	3.84e-03	8.27e-04	1.01e-04
K_{S1}	2.18e-05	5.17e-02	1.10e-03	3.55e-03	4.69e-02	1.56e-02	1.47e-02	1.12e-02	2.46e-02	1.09e-02	3.04e-03	3.96e-03	3.95e-02	2.52e-03	1.51e-02	4.80e-03	1.47e-02	1.39e-02
K_{S2}	9.69e-06	2.02e-02	4.34e-04	1.47e-03	2.00e-02	8.77e-03	5.51e-03	1.23e-02	3.23e-02	1.53e-02	3.27e-04	1.64e-03	4.26e-02	1.57e-03	1.01e-02	5.66e-03	5.47e-03	4.70e-03
K_{S3}	4.57e-06	1.94e-02	3.30e-04	1.34e-03	1.78e-02	3.38e-03	4.32e-03	2.61e-02	7.06e-03	9.30e-03	3.68e-05	1.48e-03	2.31e-03	1.03e-01	1.02e-01	3.41e-04	4.67e-03	3.85e-03
K_{S4}	6.76e-07	4.59e-03	1.79e-05	1.92e-04	2.56e-03	2.01e-04	1.87e-04	1.37e-02	1.53e-03	6.52e-03	3.46e-04	2.07e-04	3.48e-02	1.05e-01	2.71e-02	3.73e-03	9.72e-05	2.33e-05
K_{S5}	3.41e-07	3.11e-03	1.54e-05	1.96e-04	2.67e-03	6.02e-04	8.15e-05	1.36e-02	2.37e-03	4.03e-03	1.20e-04	2.11e-04	1.28e-02	1.23e-03	1.17e-01	1.66e-04	2.12e-04	1.96e-04
$K_{O,H1}$	3.76e-06	1.95e-02	1.33e-04	1.47e-04	4.98e-03	1.01e-03	2.12e-03	1.34e-02	7.67e-03	9.83e-03	9.95e-04	1.13e-04	3.98e-02	1.42e-03	8.89e-03	4.93e-03	1.01e-03	2.66e-03
$K_{O,H2}$	4.60e-06	4.84e-03	1.14e-04	1.57e-04	2.35e-03	1.29e-03	1.74e-03	8.54e-03	8.85e-03	4.31e-03	9.53e-05	1.90e-04	1.12e-03	1.53e-03	1.25e-03	1.69e-04	9.80e-04	2.08e-03
$K_{O,H3}$	1.97e-06	3.69e-03	6.16e-05	2.19e-04	2.88e-03	2.63e-04	8.89e-04	1.08e-02	1.81e-03	5.42e-03	3.34e-04	2.46e-04	3.54e-02	7.00e-02	2.79e-02	3.79e-03	8.97e-04	9.81e-04
$K_{O,H4}$	1.69e-06	8.75e-04	3.93e-05	1.05e-04	1.01e-03	1.37e-05	6.63e-04	3.79e-02	6.92e-04	3.40e-04	8.73e-05	1.07e-04	1.34e-03	5.92e-02	7.69e-03	1.92e-04	1.94e-04	8.64e-04
$K_{O,H5}$	4.93e-07	1.02e-03	2.55e-05	4.25e-05	2.03e-04	1.41e-05	4.02e-04	3.67e-02	4.77e-04	5.93e-03	5.42e-04	4.32e-05	3.37e-02	4.84e-03	3.64e-02	3.89e-03	2.73e-05	4.68e-04
K_{NO3}	2.94e-06	1.97e-03	4.71e-05	3.97e-05	3.18e-04	3.18e-05	7.88e-04	9.05e-03	3.29e-04	6.31e-03	4.09e-04	3.60e-05	3.50e-02	4.70e-03	9.68e-03	3.76e-03	2.91e-04	1.03e-03
K_{NO2}	2.26e-06	2.51e-03	1.08e-04	2.62e-04	3.63e-03	9.75e-04	1.52e-03	1.09e-02	5.90e-04	2.37e-03	3.36e-05	2.95e-04	2.15e-03	9.13e-03	1.56e-02	3.40e-04	1.37e-03	1.55e-03
K_{NO}	1.63e-06	1.73e-03	4.94e-05	5.38e-05	1.05e-03	1.35e-04	7.63e-04	3.66e-02	7.64e-04	5.53e-04	3.55e-05	6.49e-05	6.17e-04	7.55e-02	1.18e-02	2.19e-04	3.17e-04	8.69e-04
K_{N2O}	1.27e-06	1.20e-03	4.50e-05	7.09e-05	1.12e-03	4.07e-04	6.54e-04	2.00e-02	6.41e-04	1.59e-04	3.64e-05	8.22e-05	1.03e-03	2.99e-04	6.12e-02	1.90e-04	4.36e-04	7.07e-04
K_{f3NO}	1.96e-06	5.70e-04	5.35e-05	8.24e-05	9.90e-04	4.20e-04	7.97e-04	4.15e-03	4.00e-04	8.05e-03	2.80e-04	9.72e-05	4.00e-02	3.19e-03	7.24e-03	5.11e-03	8.25e-04	9.61e-04
K_{f4NO}	9.24e-07	2.52e-04	2.26e-05	7.28e-06	3.31e-05	1.45e-05	3.77e-04	1.20e-02	1.19e-04	5.24e-04	1.09e-04	3.78e-06	2.27e-03	4.34e-03	8.83e-04	3.17e-04	1.46e-04	4.93e-04
$K_{f5FNA,HET}$	1.85e-07	6.17e-04	2.67e-06	5.00e-06	1.21e-05	1.06e-04	2.86e-05	2.93e-02	4.13e-04	3.69e-04	1.16e-04	6.04e-06	1.34e-02	1.13e-03	4.03e-03	1.72e-03	2.06e-04	4.36e-05
η_{A1}	7.11e-06	1.62e-03	2.07e-04	2.34e-04	3.27e-03	1.02e-02	2.70e-03	8.77e-03	3.38e-03	2.37e-01	8.71e-05	3.00e-04	2.62e-02	3.69e-03	9.30e-03	3.76e-03	2.07e-03	2.58e-03
b_{A1}	4.37e-05	7.33e-03	8.67e-04	6.50e-04	2.05e-03	2.20e-03	1.06e-02	4.38e-02	1.14e-02	4.92e-02	1.34e-03	3.44e-04	3.09e-03	1.98e-03	6.95e-03	3.33e-04	1.09e-02	1.16e-02
Y_{A1}	5.45e-05	1.86e-03	3.56e-03	2.98e-03	5.10e-02	8.08e-02	4.68e-02	3.52e-02	4.75e-03	2.14e-01	2.62e-03	3.57e-03	2.42e-03	6.47e-03	9.65e-04	4.20e-04	4.83e-02	4.57e-02
K_{OA1}	1.03e-05	7.23e-04	3.06e-04	3.66e-04	5.21e-03	3.33e-03	3.93e-03	2.26e-02	2.39e-03	2.46e-01	7.97e-04	4.28e-04	1.90e-02	3.05e-03	5.69e-03	3.72e-03	2.89e-03	3.90e-03

	S_I	S_S	X_I	X_S	X_H	X_{AOB}	X_P	S_O	S_{NO3}	S_{NH4}	S_{ND}	X_{ND}	S_{NO2}	S_{NO}	S_{N2O}	S_{N2}	X_{NOB}	X_{AMX}
K_{FA}	4.99e-07	1.20e-03	1.82e-04	3.69e-05	9.86e-04	4.10e-03	2.65e-03	5.09e-02	1.48e-03	1.01e-01	2.55e-04	7.49e-05	3.65e-02	5.00e-03	9.70e-03	3.99e-03	1.65e-03	3.07e-03
K_{I9FA}	9.34e-07	1.00e-03	1.90e-05	1.24e-05	2.64e-06	7.28e-04	2.82e-04	3.73e-02	9.59e-04	2.06e-02	1.73e-04	1.79e-05	3.88e-02	3.49e-03	1.01e-02	5.29e-03	2.65e-04	3.27e-04
K_{I9FNA}	6.94e-07	1.21e-03	1.19e-05	1.70e-05	1.01e-04	1.23e-05	2.06e-04	5.25e-02	4.12e-04	9.12e-03	1.59e-04	1.65e-05	3.85e-02	3.68e-03	1.01e-02	5.19e-03	5.62e-05	2.60e-04
η_{A2}	2.45e-06	1.84e-03	9.56e-06	2.62e-04	3.59e-03	3.84e-03	6.62e-04	1.83e-02	3.56e-02	2.38e-02	4.06e-04	2.76e-04	6.53e-03	2.52e-03	1.97e-03	1.48e-03	4.22e-02	1.58e-03
b_{A2}	1.63e-06	1.09e-04	6.48e-06	3.59e-05	1.35e-04	3.75e-04	2.02e-04	2.76e-02	2.41e-03	2.61e-03	4.71e-05	3.18e-05	1.25e-02	6.75e-04	3.63e-03	1.58e-03	9.96e-03	2.72e-04
Y_{A2}	7.34e-06	4.13e-04	1.46e-04	2.24e-05	5.00e-04	2.82e-03	2.18e-03	6.94e-03	3.04e-02	1.48e-02	1.15e-04	3.64e-06	4.85e-03	1.51e-03	1.80e-03	4.89e-03	8.89e-04	2.62e-03
K_{OA2}	3.30e-06	3.32e-04	1.18e-04	7.34e-05	1.54e-03	3.15e-03	1.57e-03	2.46e-02	2.78e-02	1.45e-02	9.08e-05	9.86e-05	2.77e-03	9.86e-04	1.37e-03	4.55e-04	2.58e-02	1.63e-03
K_{FNA}	3.46e-06	1.67e-03	7.90e-05	3.21e-05	1.38e-04	6.95e-04	1.24e-03	6.88e-03	5.76e-03	9.32e-03	4.39e-04	2.08e-05	4.02e-02	3.81e-03	1.00e-02	5.01e-03	6.52e-03	1.58e-03
K_{I10FA}	2.10e-06	1.33e-03	3.62e-05	2.23e-05	2.04e-04	1.05e-04	5.94e-04	4.30e-03	2.89e-04	6.22e-03	1.42e-04	1.80e-05	3.31e-02	4.20e-03	9.61e-03	3.90e-03	3.32e-04	7.87e-04
K_{I10FNA}	5.09e-07	1.82e-03	6.16e-06	1.44e-05	9.56e-05	7.54e-05	1.13e-04	1.32e-02	3.24e-04	6.52e-03	3.41e-04	1.48e-05	3.53e-02	4.80e-03	9.83e-03	3.73e-03	7.24e-05	1.35e-04
η_{AMX}	1.38e-06	5.43e-03	7.48e-05	7.63e-04	9.05e-03	3.13e-03	2.70e-04	2.18e-02	3.71e-03	8.75e-03	1.09e-04	7.98e-04	6.40e-02	8.64e-03	2.44e-02	2.29e-03	7.95e-04	4.55e-04
b_{AMX}	1.78e-05	1.21e-03	8.89e-05	6.73e-05	1.61e-03	4.52e-04	1.27e-03	1.20e-02	1.84e-03	1.57e-03	5.01e-04	9.80e-05	2.17e-03	8.81e-04	1.85e-03	2.27e-04	6.81e-04	2.06e-03
Y_{AMX}	1.26e-04	2.19e-03	6.49e-04	2.42e-04	1.03e-03	6.88e-03	9.60e-03	2.84e-02	8.94e-02	3.60e-02	7.47e-04	1.64e-04	5.00e-02	4.47e-03	1.69e-02	2.51e-03	4.44e-03	1.18e-02
$K_{O2,AMX}$	2.11e-06	6.49e-04	4.36e-05	1.57e-04	1.67e-03	3.87e-04	8.69e-04	1.79e-02	1.23e-03	3.00e-03	1.98e-04	1.53e-04	1.62e-02	9.27e-04	4.38e-03	1.80e-03	3.79e-04	1.30e-03
$K_{NH,AMX}$	2.57e-07	3.32e-04	8.28e-06	1.67e-05	1.87e-04	9.02e-05	1.12e-04	5.77e-03	1.24e-04	2.71e-03	3.21e-05	1.85e-05	1.38e-02	7.45e-04	3.94e-04	1.50e-03	6.32e-05	1.31e-04
$K_{NO2,AMX}$	1.95e-06	2.14e-03	1.08e-04	2.74e-04	3.54e-03	1.24e-03	1.42e-04	2.12e-02	1.01e-03	4.90e-03	2.71e-04	3.00e-04	3.49e-02	3.15e-03	1.36e-02	1.59e-03	5.40e-04	1.50e-03
L_{max}	1.73e-03	1.38e-02	5.06e-02	6.16e-02	6.64e-01	6.36e-01	6.86e-01	1.84e-01	4.14e-02	2.24e-01	2.34e-02	7.23e-02	3.96e-02	1.09e-01	6.04e-03	3.26e-03	6.52e-01	6.93e-01
L_0	3.47e-05	1.75e-02	1.04e-03	7.59e-05	7.69e-05	2.07e-02	1.51e-02	5.20e-02	9.47e-02	6.41e-01	2.39e-03	8.25e-05	5.69e-02	1.27e-02	3.74e-02	5.42e-02	2.77e-02	1.71e-02
ρ	6.18e-03	8.56e-03	5.51e-02	5.37e-02	6.74e-01	6.42e-01	6.96e-01	5.07e-01	3.31e-02	2.20e-01	2.31e-02	6.38e-02	1.07e-01	7.06e-02	2.79e-02	7.57e-03	6.59e-01	7.03e-01
η	6.18e-03	8.56e-03	5.51e-02	5.37e-02	6.74e-01	6.42e-01	6.96e-01	5.07e-01	3.31e-02	2.20e-01	2.31e-02	6.38e-02	1.07e-01	7.06e-02	2.79e-02	7.57e-03	6.59e-01	7.03e-01
k_{Att}	1.53e-05	2.93e-03	5.22e-03	7.76e-03	1.41e-02	9.39e-03	1.13e-02	2.34e-02	1.41e-03	8.90e-03	1.41e-03	7.89e-03	3.86e-02	2.19e-03	9.80e-03	5.04e-03	9.76e-03	1.10e-02
k_{Det}	5.57e-05	8.81e-04	1.43e-03	2.16e-03	1.76e-02	1.64e-02	2.03e-02	2.09e-02	1.56e-03	6.19e-03	4.99e-04	2.51e-03	1.64e-02	9.38e-04	4.72e-03	2.57e-03	1.76e-02	2.13e-02
D_X	7.61e-06	4.14e-03	5.52e-05	1.48e-04	3.35e-03	4.80e-03	1.34e-03	1.95e-02	6.69e-03	2.63e-02	5.91e-04	2.00e-04	1.21e-02	2.04e-03	2.93e-03	1.35e-03	5.66e-03	2.70e-03
D_{SI}	1.67e-06	2.58e-04	3.85e-05	4.75e-05	4.31e-04	1.86e-06	6.57e-04	3.27e-02	5.37e-04	9.70e-04	6.03e-05	4.46e-05	7.32e-04	1.94e-04	2.27e-04	2.53e-04	2.64e-04	8.76e-04
D_{SS}	1.70e-06	3.02e-03	4.56e-05	2.14e-04	2.61e-03	5.86e-04	6.32e-03	2.52e-02	7.93e-04	6.50e-04	3.15e-05	2.39e-04	7.34e-04	9.04e-04	4.11e-04	2.30e-04	7.61e-04	6.80e-04
D_{O2}	3.99e-05	1.42e-02	1.20e-04	4.88e-04	1.11e-02	3.52e-02	8.39e-04	1.95e-02	9.99e-02	2.64e-01	3.32e-03	6.60e-04	1.24e-02	1.95e-02	4.03e-02	4.49e-02	1.50e-02	9.39e-05
D_{NO3}	8.15e-07	2.51e-04	2.92e-05	1.20e-05	1.37e-04	1.06e-04	4.66e-04	4.04e-02	4.53e-04	2.48e-03	2.95e-04	7.48e-06	1.28e-02	6.92e-04	3.68e-03	1.47e-03	2.75e-04	6.33e-04
D_{NH4}	2.56e-06	2.50e-03	5.62e-05	6.32e-05	6.55e-04	3.68e-03	9.49e-04	1.02e-02	1.40e-03	3.59e-03	2.11e-04	5.59e-05	1.37e-02	7.98e-04	4.01e-03	1.41e-03	5.52e-04	1.31e-03
D_{SND}	8.30e-07	1.09e-03	2.23e-06	9.32e-07	1.99e-05	1.10e-05	4.31e-05	8.28e-03	4.32e-04	8.69e-03	1.25e-03	1.80e-06	3.92e-02	3.55e-03	1.01e-02	5.14e-03	3.33e-05	6.83e-05
D_{NO2}	1.71e-06	2.23e-03	3.89e-05	8.70e-05	9.00e-04	2.28e-03	1.58e-04	4.04e-02	3.33e-03	6.65e-03	9.66e-05	8.04e-05	7.69e-02	1.11e-02	1.21e-02	2.18e-02	5.39e-03	1.62e-04
D_{NO}	1.90e-06	1.88e-03	3.89e-05	7.35e-05	7.97e-04	1.07e-04	6.36e-04	2.07e-02	4.96e-04	8.52e-03	2.04e-04	7.24e-05	3.98e-02	4.01e-02	1.09e-02	5.25e-03	4.05e-04	8.73e-04
D_{N2O}	2.28e-06	8.36e-04	4.27e-05	1.29e-04	1.42e-03	2.16e-04	7.81e-04	2.56e-02	8.50e-04	1.72e-03	1.71e-04	1.29e-04	8.84e-03	9.91e-04	2.23e-02	1.86e-03	2.19e-04	1.16e-03
D_{N2}	3.95e-07	1.74e-03	2.65e-05	1.12e-04	1.60e-04	6.34e-04	2.57e-04	8.54e-03	1.50e-03	3.79e-03	3.18e-05	1.17e-04	2.06e-02	2.50e-03	4.43e-03	2.96e-03	3.10e-04	6.78e-05
$K_{FA,AD}$	4.73e-07	1.83e-03	1.58e-05	2.67e-05	2.71e-04	1.40e-04	2.94e-04	9.19e-03	3.87e-04	6.28e-03	4.76e-04	2.61e-05	3.52e-02	3.86e-03	9.78e-03	3.70e-03	7.39e-05	3.91e-04
$K_{FNA,AOB}$	7.85e-07	1.11e-03	2.88e-06	4.27e-06	6.33e-05	3.56e-05	4.82e-05	1.31e-02	6.51e-04	7.34e-03	1.92e-04	3.74e-06	3.29e-02	4.26e-03	9.53e-03	3.96e-03	7.93e-05	7.27e-05
f_B	2.60e-06	4.13e-04	6.04e-05	6.21e-05	4.20e-04	5.19e-05	1.00e-03	4.42e-02	4.15e-04	6.01e-04	2.07e-05	5.66e-05	8.56e-04	4.36e-04	2.98e-04	2.26e-04	3.74e-04	1.33e-03

	S_I	S_S	X_I	X_S	X_H	X_{AOB}	X_P	S_O	S_{NO3}	S_{NH4}	S_{ND}	X_{ND}	S_{NO2}	S_{NO}	S_{N2O}	S_{N2}	X_{NOB}	X_{AMX}
$f_{DNT,A}$	8.04e-07	1.65e-03	1.86e-06	3.64e-06	2.11e-05	4.94e-05	2.45e-05	1.42e-02	4.33e-04	8.75e-03	3.14e-04	4.62e-06	4.04e-02	4.11e-06	1.01e-02	5.09e-03	8.77e-05	4.37e-05
$K_{NO,AOB}$	2.72e-07	4.52e-04	9.43e-06	8.91e-07	1.20e-04	3.55e-05	1.61e-04	1.13e-02	4.27e-04	2.98e-03	5.71e-05	1.87e-06	1.41e-02	1.24e-03	4.01e-03	1.64e-03	1.28e-04	2.36e-04

Table B.1: Full sensitivity analysis results. Percentage difference (absolute value) in the outputs when the parameter value is increased with 10% from its nominal value.